Supramolecular Assembly of Tris(4-carboxyphenyl)arenes: Relationship between Molecular Structure and Solid-State Catenation Motifs

Holden W. H. Lai[†,*], Ren A. Wiscons[†], Cassandra A. Zentner[†], Matthias Zeller[‡], Jesse L. C. Rowsell[†]

[†]Department of Chemistry and Biochemistry, Oberlin College, 119 Woodland Street, Oberlin, OH 44074, USA

[‡]Department of Chemistry, Youngstown State University, One University Plaza, Youngstown, OH 44555, USA

Table of Contents

Additional Notes

Note 1: The structures of **1** and **9** have been previously described as 8-fold polycatenated and 6-fold interpenetrated. The terminology used here describe the same catenation motifs as DOC = (7/7) and (6/6), respectively.

Note 2: Steric A values are empirical measures of the steric demand of a functional group, based on how the functional group affects the conformation of cyclohexane. For instance, an A value of 0.6 kcal/mol for the methoxy group indicates that for methoxycyclohexane, the conformation with the methoxy group in the axial position is 0.6 kcal/mol higher in energy than the conformation with the methoxy group in the equatorial position.

SC-XRD Special Experimental Details

Data for compound **5** were collected through Service Crystallography at the Advanced Photon Source at Beamline 15-ID B ChemMatCARS (λ = 0.41328) with a Bruker AXS APEXII CCD diffractometer. Data of **8** and the homo coupling product dimethyl biphenyl-4,4'-dicarboxylate were collected on a Bruker AXS APEXII CCD diffractometer with a sealed tube X-ray source with graphite monochromated molybdenum radiation (λ = 0.71073 Å). Single crystal data for all other compounds were collected using either a Bruker AXS X8 Prospector CCD diffractometer with a copper I-μ-S microsource X-ray tube (λ = 1.54178 Å) (**2**, **3**, **4**, intermediate 2,4,6-tris(4-carboxyphenyl)anisole trimethyl ester), or a Bruker AXS D8 Quest CMOS diffractometer with a molybdenum I-μ-S microsource X-ray tube (λ = 0.71073 Å) (**6**, **7**, intermediates 2,4,6-tris(4-carboxyphenyl)aniline trimethyl ester, 2,4,6-tritolylnitrobenzene). The Prospector and Quest diffractometers feature laterally graded multilayer (Goebel) mirrors for monochromatization. Single crystals were mounted on Mitegen micromesh mounts with the help of a trace of oil and flash cooled to either 200 K and further cooled at 5 degree per minute to 100 K where crystals withstood further cooling (otherwise data were collected at 200 K). The Apex2 software package was used to determine unit cells and for data collection, and data were integrated using SAINT. The data were processed with SADABS and corrected for absorption using multi-scan techniques. The space groups were assigned using XPREP of the Bruker SHELXTL package, solved with ShelXD, and refined with SHELXL 2013 or 2014 and the graphical interface Shelxle. All non-hydrogen atoms were refined anisotropically. H atoms attached to carbon, nitrogen and hydroxyl oxygen atoms were positioned geometrically and constrained to ride on their parent atoms, with carbon hydrogen bond distances of 0.95 Å for aromatic C-H, 0.99 and 0.98 Å for aliphatic CH_2 and CH_3 and 0.88 Å for NH_2 moieties, and 0.84 Å for carboxylic acid moieties, respectively. Hydroxyl and methyl H atoms were allowed to rotate but not to tip to best fit the experimental electron density. U_{iso}(H) values were set to a multiple of U_{eq}(C/O/N) with 1.5 for O-H and CH_3, and 1.2 for C-H and N-H, respectively. All structures feature large solvent accessible volumes within their rigid frameworks. The contents of these volumes are highly disordered and the residual electron density peaks are not arranged in an interpretable pattern. The hkl files were thus corrected for using reverse Fourier transform methods using the SQUEEZE routine (P. van der Sluis & A.L. Spek (1990). Acta Cryst. A46, 194-201) as implemented in the program Platon (Version 191114, Feb 10. 2015). The resultant files were used in the further refinement. (The FAB files with details of the Squeeze results are appended to the cif files). Additional details are presented in Table 1 of the main manuscript, in Table S1 for structures of intermediates, and are given as Supporting

Information in the CIF files. Complete crystallographic data, in CIF format, have been deposited with the Cambridge Crystallographic Data Centre. CCDC 1422491-1422501 contain the supplementary crystallographic data for this paper. These data can be obtained free of charge from The Cambridge Crystallographic Data Centre via www.ccdc.cam.ac.uk/data_request/cif.

Crystals of **2** did not survive cooling to 100 K and data were thus collected at 200 K. The structure contains four independent solvent accessible voids of 501 $Å^3$ each per unit cell. The residual electron density peaks are not arranged in an interpretable pattern, with intensities of two electrons per cubic Ångström or less. The hkl file was thus corrected for using reverse Fourier transform methods using the SQUEEZE routine, which corrected for 139 electrons within each of the solvent accessible voids.

The structure of **3** contains substantial solvent accessible voids (77.0 % of the unit cell volume (two areas of 13438 $Å^3$ each) calculated using the SQUEEZE procedure and 69 % of the unit cell volume calculated using CCDC Mercury computer software, with a probe radius of 1.2 Å and approximate grid spacing of 0.7 Å). The largest part consists of highly disordered ill-defined solvate molecules with residual electron density peaks not arranged in an interpretable pattern. Small areas close to the main lattice molecules were recognizable as acetonitrile and 1,4-dioxane molecules (weakly H bonded to C-H units of the benzene rings and thus better defined). Due to the ill resolution of these solvent molecules, ultimately all content of these voids was ignored and the hkl file was instead corrected for using reverse Fourier transform methods using the SQUEEZE routine, which corrected for 3424 electrons within the solvent accessible voids.

The structure of **4** exhibits pseudo-inversion symmetry (emulating space group Pbcn) broken by ordering of the positions of carboxylic acid hydrogen atoms and single/double bond locations. Refinement in a centrosymmetric setting yielded R values doubled in value (R1 ca. 18%). Atom thermal parameters are correlated due to the pseudo-inversion center. Atoms related by pseudosymmetry were constrained to have identical ADPs. For one pair of carboxylate groups (that of O3/O4 of the A and B moieties, the double and single C-O bonds in both moieties were restrained to have similar bond lengths each. Carboxylic acid H atoms were restrained to lie in one plane with their carboxylate group C and O atoms. The structure was refined as a 2-component inversion twin, Flack parameter 0.5(4).
The structure contains solvent accessible voids of combined 3820.6 $Å^3$. The residual electron density was recognizable as heavily disordered dioxane and potentially other solvate molecules but no suitable disorder model could be developed due to partial occupancy, disorder, partially not recognizable disordered moieties, and correlation of moieties related by pseudosymmetry. The hkl file was thus corrected for using reverse Fourier transform methods using the SQUEEZE routine, which corrected for 1179.2 electrons within the solvent accessible voids.

The structure of **5** contains solvent accessible voids of 6691.3 $Å^3$. No substantial electron density peaks were found in the solvent accessible voids (less than 1.5 electron per cubic Ångström) and the residual electron density peaks are not arranged in an interpretable pattern. The hkl file was thus corrected for using reverse Fourier transform methods using the SQUEEZE routine, which corrected for 2053.4 electrons within the solvent accessible voids.
Carboxylic acid H atoms were placed in calculated positions (AFIX 147) with a possibility to rotate around the C-O bond, but were restrained to lie within the plane of the carboxylate C and O

atoms. Carboxylic acid H atoms attached to O3A, O3B and O3C were set as half occupied due to disorder of C-OH with C=O moieties. Reflection 2 0 0 was affected by the beam stop and was omitted from the refinement.

In the structure of **6** one methyl and one amino substituent attached to the central benzene rings were refined as disordered over all possible positions. Equivalent 1,2 and 1,3 distances involving the methyl C and amino N atoms were restrained to be similar (SADI restraints in Shelxl). Overlapping C and N atoms were constrained to have identical ADPs. The least occupied methyl C and amino N atoms were constrained to have the same ADP as that of the neighboring benzene C atom. Amino H atoms, with the exception of those attached to the least most occupied one, were restrained to have N-H bond distances of 0.88(2) Å, and H...H distances of 1.524(20) Å. All other H atoms were placed in calculated positions in the usual manner.
Subject to these conditions the occupancies of the three amino groups refined to 0.6718(19), 0.3020(19) and 0.0262(19) for N1, N2 and N3, respectively. Occupancies of C28A, C28B and C28C refined to 0.2983(19), 0.6845(19) and 0.0172(19), respectively.
The structure contains 4 equivalent solvent accessible voids of 300 $Å^3$ each. No interpretable electron density was found in the solvent accessible voids. The hkl file was thus corrected for using reverse Fourier transform methods using the SQUEEZE routine, which corrected for 78 electrons within each of the solvent accessible voids.

In the structure of **7** two amino substituents attached to the central benzene rings were refined as disordered over all possible positions. Equivalent C-N bond distances were restrained to be similar (SADI command in SHELXL). Amino H atoms, with the exception of those attached to the least occupied one, were restrained to have N-H bond distances of 0.88(2) Å, and H...H distances of 1.524(20) Å. All other H atoms were placed in calculated positions in the usual manner. Subject to these conditions the occupancies of the three amino groups refined to 0.877(3), 0.923(3) and 0.200(2) for N1, N2 and N3, respectively.
The structure contains 4 equivalent solvent accessible voids of 282 $Å^3$. No interpretable electron density was found in the solvent accessible voids. The hkl file was thus corrected for using reverse Fourier transform methods using the SQUEEZE routine, which corrected for 67 electrons within each of the solvent accessible voids.

Large sections of the structure of **8** are occupied by disordered solvate molecules. The overall disorder did not allow for definition of a satisfactory solvate molecule model, and the electron density for the solvate molecules was instead corrected for by reverse Fourier transform methods using the Squeeze procedure. 245 electrons from 1315 $Å^3$ of volume (ca 38.6% of the unit cell volume) were corrected for.
The structure exhibits approximate mirror and inversion symmetry (Ibam), broken by the tilt angle of the ring C14B to C19B and that of the connected carboxylic acid group. All attempts to refine the structure in this higher symmetry resulted in substantially higher R value (R1>70%), non-positive ADPs for all atoms, and an unstable refinement.
Due to the overall low quality of the data, a rigid bond restraint (RIGU 0.03) was applied for all atoms. A nitro group is disordered over two pseudo-mirror symmetry related positions. C-N distances of the two disordered groups were restrained to be similar to those of the not disordered third nitro group, distances of nitro O atoms to second next neighbors to be similar, and all nitro groups were restrained to be flat. Disordered pseudo-equivalent nitro N atoms were constrained to

have identical ADPs. Disordered nitro O atoms were restrained to be approximately isotropic. Subject to these conditions the occupancy ratio refined to 0.538(13) to 0.462(13). All C-C bonds between carboxylate C and adjacent phenyl C atoms were restrained to be similar. Two benzene rings (C13A to C26A and C7B to C12B) were constrained to resemble ideal hexagons with C-C distances of 1.39 Å. Atoms C2B, O5B and O6B were also restrained to be approximately isotropic. Distances of carboxylate dimer H-bonds were restrained to 1.80(2) Å. One hydroxyl atom, H3B1, was set to ride on the carrying O atom in the final refinement cycles. Several low angle diffraction spots were affected by the beam stop and were omitted from the refinement. The reflections omitted are 1 1 0, 0 2 -2, 0 2 2, 0 2 0, 0 0 2, 1 2 -3, 0 4 0 and 1 1 2.

Table S1. Experimental details for intermediates and side products

Experiments were carried out at 100 K. Data collection used ω and phi scans. H-atom parameters were constrained.

	2,4,6-tris(4-carboxyphenyl)aniline trimethyl ester	2,4,6-tris(4-carboxyphenyl)anisole trimethyl ester	2,4,6-tritolylnitrobenzene	dimethyl biphenyl-4,4'-dicarboxylate
Crystal data				
Chemical formula	$C_{30}H_{25}NO_6$	$C_{31}H_{26}O_7$	$C_{27}H_{23}NO_2$	$C_{16}H_{14}O_4$
M_r	495.51	510.52	393.46	270.27
Crystal system, space group	Orthorhombic, *Pbcn*	Monoclinic, $P2_1/c$	Orthorhombic, *Pbca*	Orthorhombic, *Pbca*
a, *b*, *c* (Å)	24.2244 (10), 7.7980 (4), 26.5186 (11)	12.6185 (4), 22.3524 (8), 9.6909 (3)	12.7521 (4), 12.5544 (4), 26.1460 (8)	7.1095 (7), 5.9603 (6), 29.678 (3)
α, β, γ (°)	90, 90, 90	90, 109.558 (1), 90	90, 90, 90	90, 90, 90
V (Å^3)	5009.4 (4)	2575.65 (15)	4185.8 (2)	1257.6 (2)
Z	8	4	8	4
F(000)	2080	1072	1664	568
D_x (Mg m^{-3})	1.314	1.317	1.249	1.427
Radiation type	Mo *K*α	Cu *K*α	Mo *K*α	Mo *K*α
No. of reflections for cell measurement	7419	9987	6753	2098
θ range (°) for cell measurement	3.0–28.2	3.7–66.7	2.8–28.3	2.7–31.3
μ (mm^{-1})	0.09	0.77	0.08	0.10
Crystal shape	Plate	Needle	Rod	Plate
Colour	Yellow	Colourless	Colourless	Colourless
Crystal size (mm)	0.37 × 0.15 × 0.05	0.33 × 0.14 × 0.09	0.55 × 0.14 × 0.04	0.50 × 0.29 × 0.09
Data collection				
Diffractometer	Bruker AXS D8 Quest CMOS diffractometer	Bruker AXS Prospector CCD diffractometer	Bruker AXS D8 Quest CMOS diffractometer	Bruker AXS APEXII CCD diffractometer
Radiation source	I-mu-S microsource X-ray tube	I-mu-S microsource X-ray tube	I-mu-S microsource X-ray tube	fine focus sealed tube
Monochromator	Laterally graded multilayer (Goebel) mirror	Laterally graded multilayer (Goebel) mirror	Laterally graded multilayer (Goebel) mirror	Graphite
Absorption correction	Multi-scan Apex2 v2014.1-1 (Bruker, 2014)	Multi-scan Apex2 v2014.1-0 (Bruker, 2014)	Multi-scan Apex2 v2014.1-1 (Bruker, 2014)	Multi-scan Apex2 v2013.4-1 (Bruker, 2013)
T_{min}, T_{max}	0.577, 0.746	0.442, 0.753	0.684, 0.746	0.596, 0.746
No. of measured, independent and observed [$I > 2\sigma(I)$] reflections	25163, 5986, 4212	21395, 4497, 4233	18287, 5161, 4062	4374, 1860, 1601
R_{int}	0.069	0.052	0.033	0.016
θ values (°)	θ_{max} = 28.3, θ_{min} = 2.9	θ_{max} = 66.8, θ_{min} = 3.7	θ_{max} = 28.3, θ_{min} = 2.2	θ_{max} = 31.3, θ_{min} = 1.4
$(\sin\theta/\lambda)_{max}$ (Å^{-1})	0.667	0.596	0.667	0.731
Range of *h*, *k*, *l*	*h* = -31→32, *k* = -10→9, *l* = -35→35	*h* = -14→14, *k* = -26→26, *l* = -11→11	*h* = -16→11, *k* = -16→13, *l* = -34→33	*h* = -9→8, *k* = -8→8, *l* = -42→15
Refinement				
$R[F^2 > 2\sigma(F^2)]$, $wR(F^2)$, *S*	0.080, 0.163, 1.13	0.048, 0.133, 1.03	0.044, 0.112, 1.02	0.046, 0.129, 1.07

No. of reflections	5986	4497	5161	1860
No. of parameters	337	348	274	92
$\Delta\rho_{max}$, $\Delta\rho_{min}$ (e Å^{-3})	0.36, -0.28	0.30, -0.32	0.35, -0.22	0.65, -0.25

Computer programs: Apex2 v2014.1-1 (Bruker, 2014), Apex2 v2014.1-0 (Bruker, 2014), Apex2 v2013.4-1 (Bruker, 2013), *SAINT* V8.34A (Bruker, 2014), *SAINT* V8.30C (Bruker, 2013), *SHELXS97* (Sheldrick, 2008), *SHELXL2013* (Sheldrick, 2013), SHELXLE Rev645 (Hübschle *et al.*, 2011).

ORTEP Plots

Thermal ellipsoid levels are at the 50% probability level for all compounds.

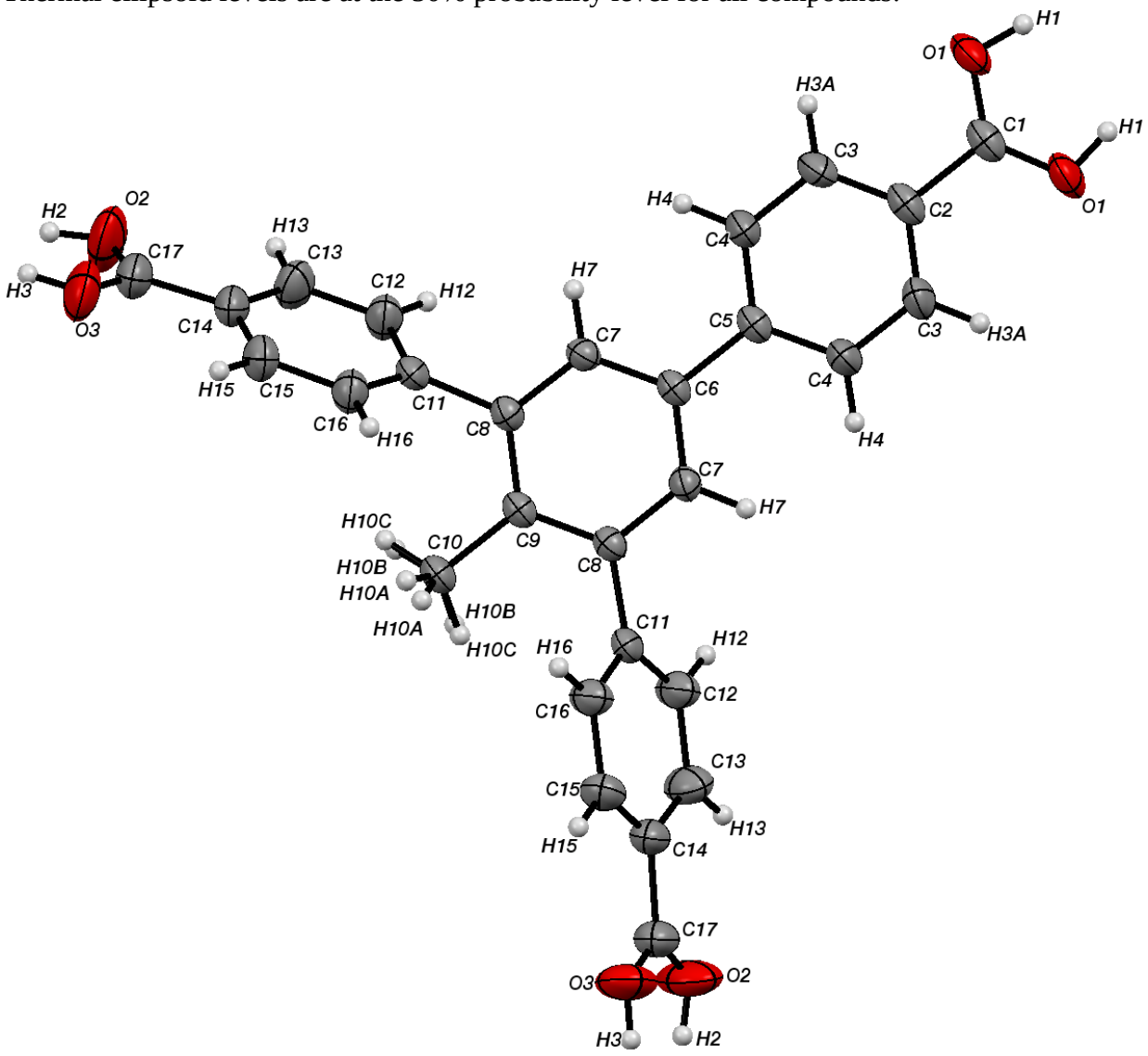

Figure S1.ORTEP-style plot of compound **2**. Hydrogen atoms at oxygen atoms and at the methyl group are disordered due to a mirror plane bisecting the molecule, or due to non-systematic disorder (H atoms attached to O2 and O3).

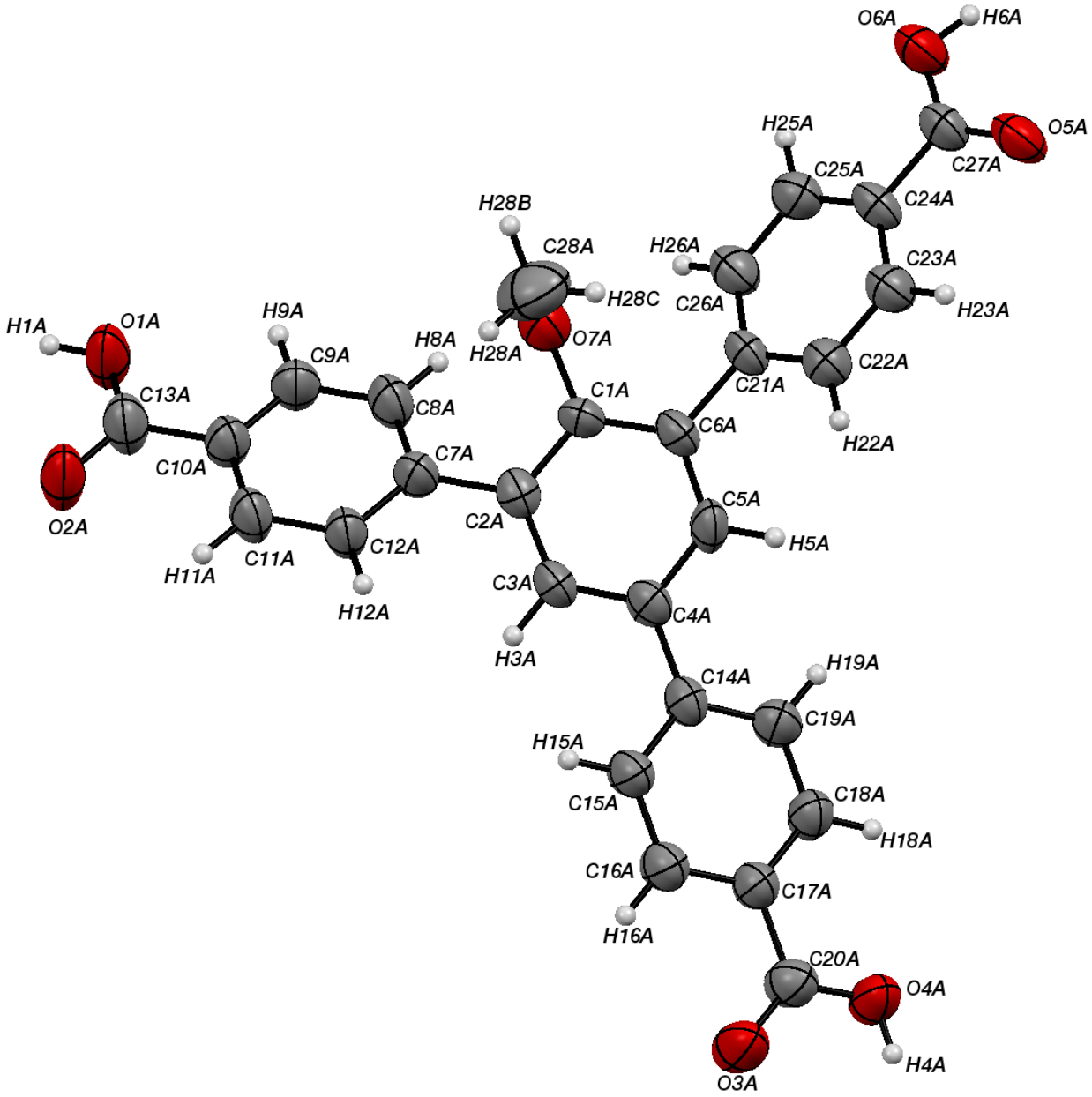

Figure S2a. ORTEP plot of the first of the three crystallographically independent molecules in the asymmetric unit of compound **3**.

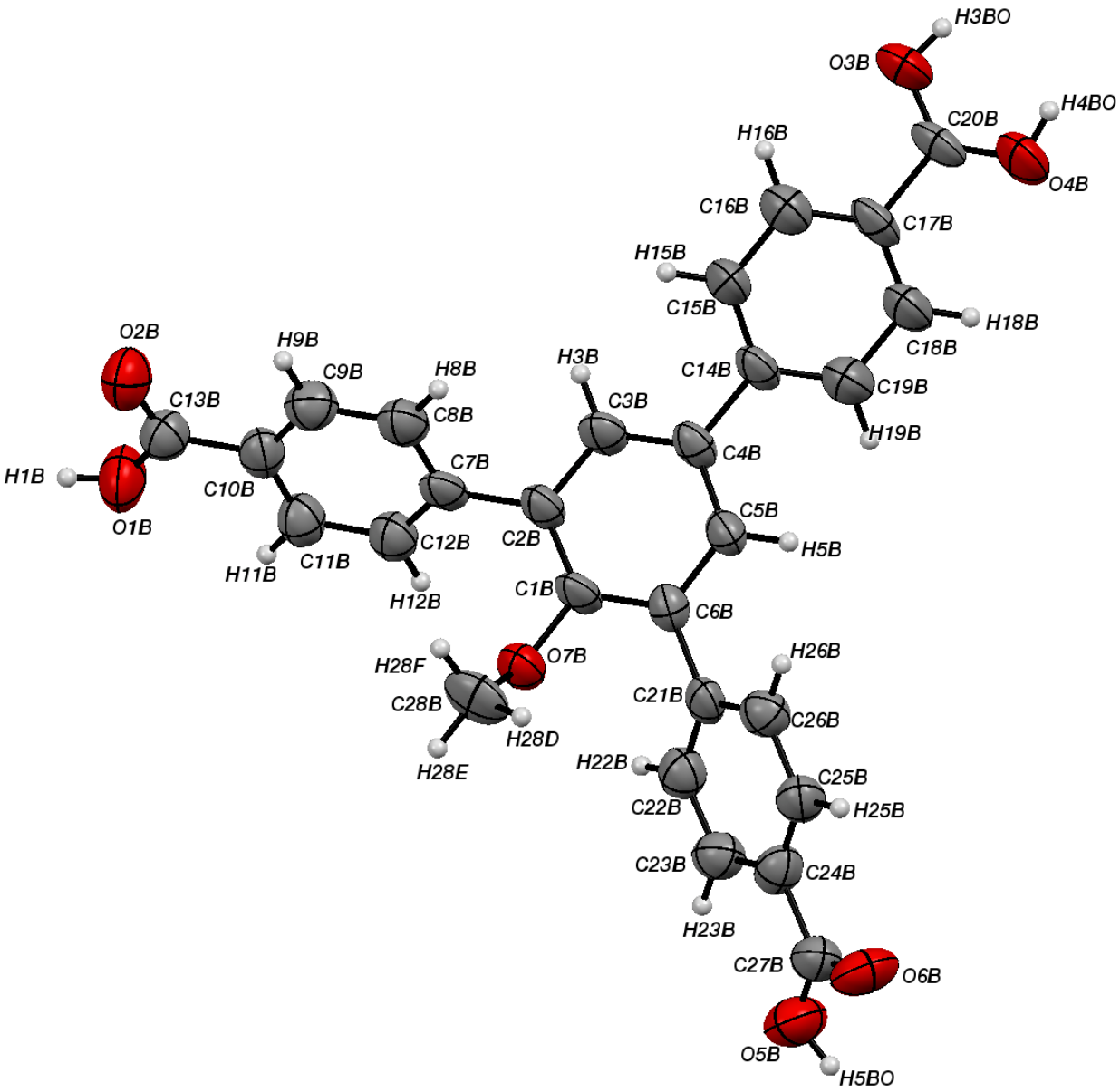

Figure S2b. ORTEP plot of the second of the three crystallographically independent molecules in the asymmetric unit of compound **3**.

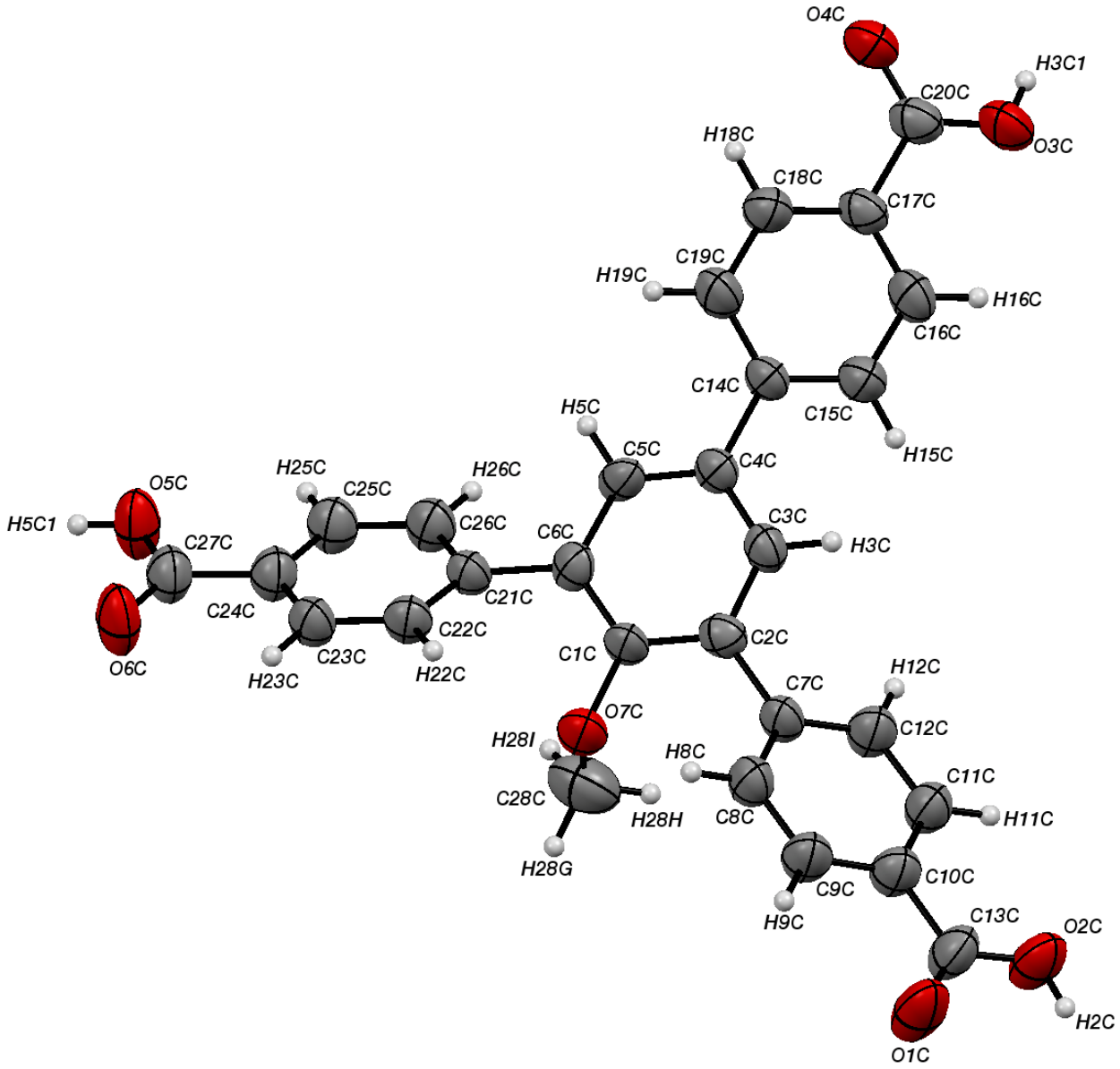

Figure S2c. ORTEP plot of the third of the three crystallographically independent molecules in the asymmetric unit of compound **3**.

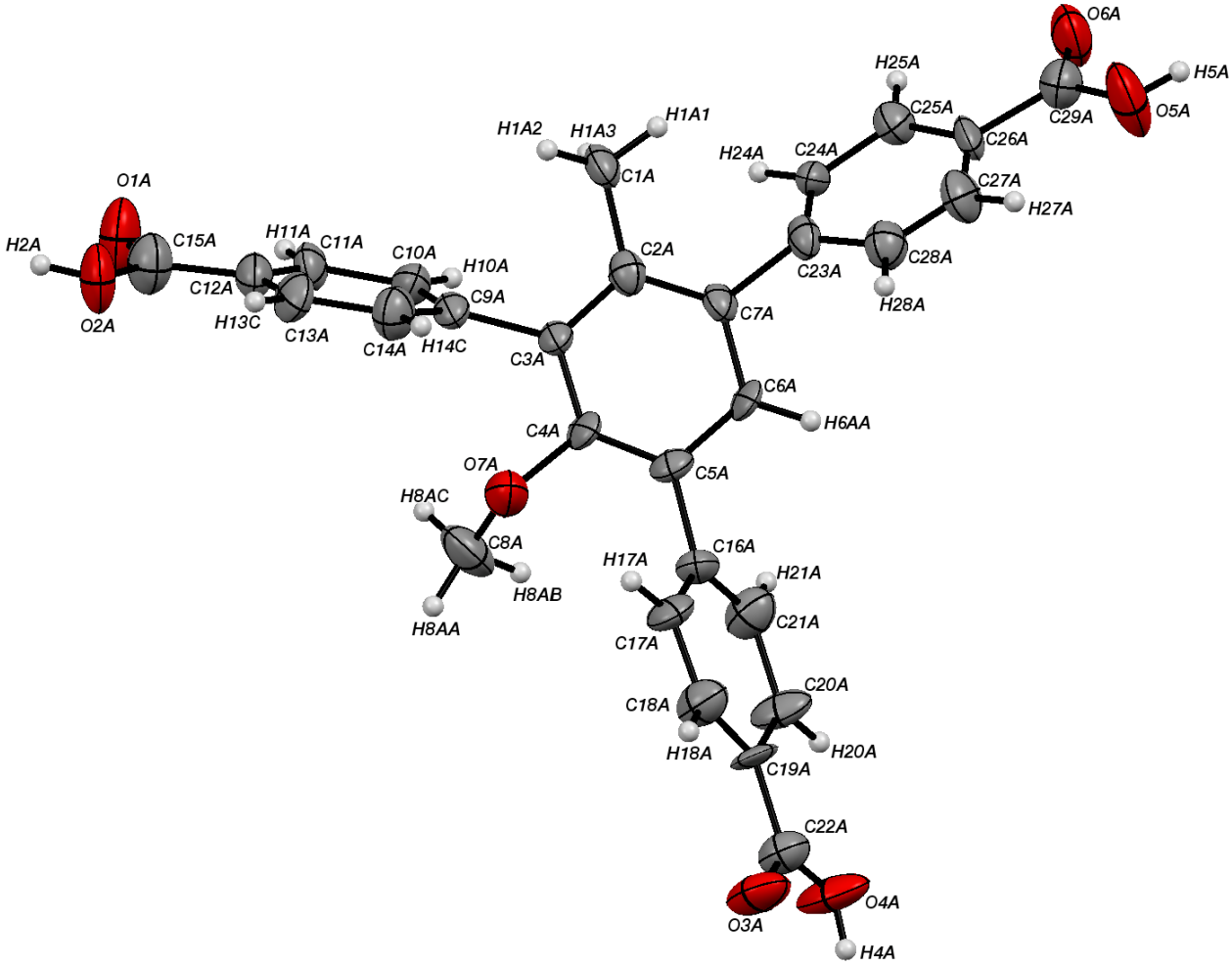

Figure S3a. ORTEP plot of the first of the two crystallographically independent molecules in the asymmetric unit of compound **4**.

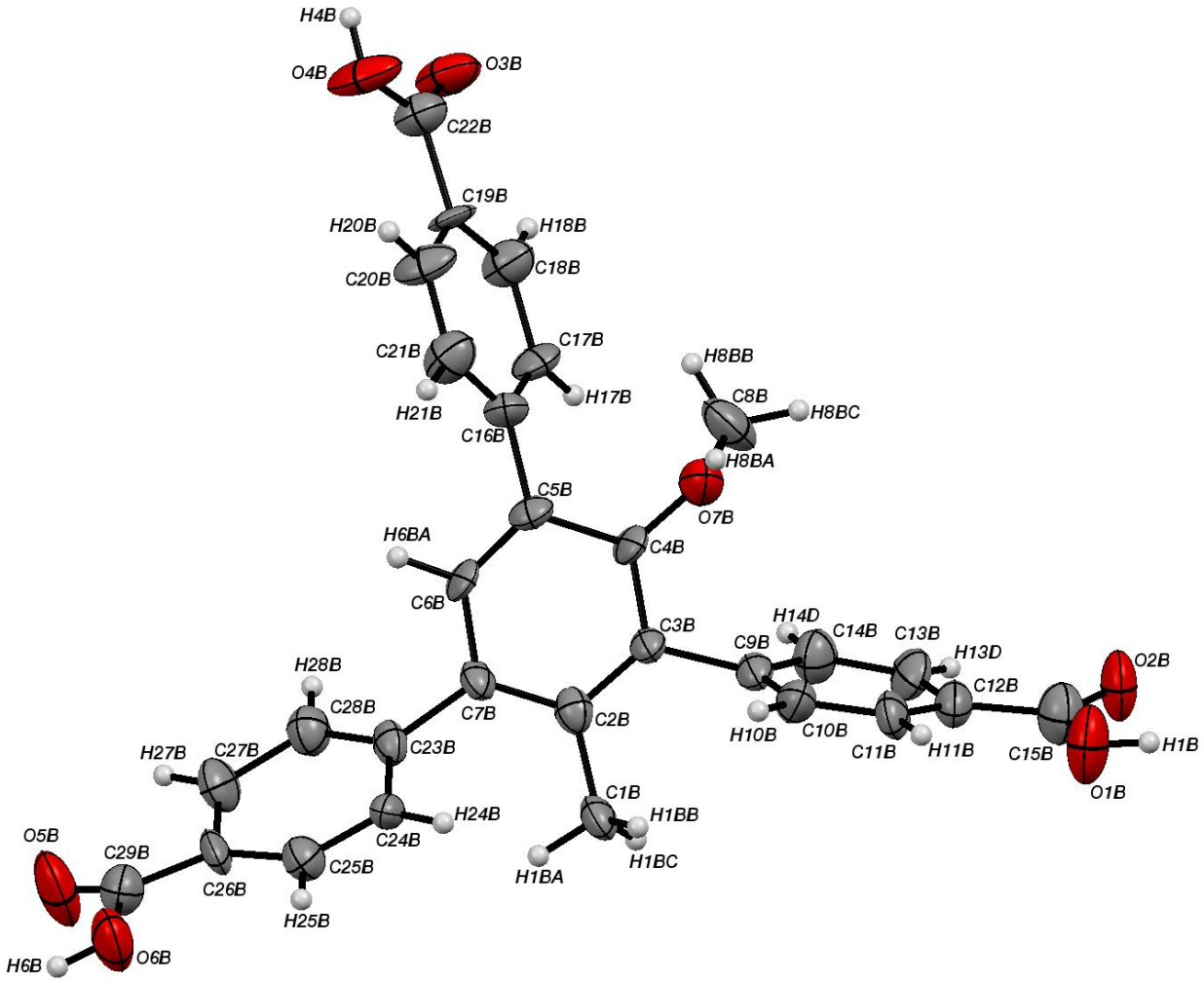

Figure S3b.ORTEP plot of the second of the two crystallographically independent molecules in the asymmetric unit of compound **4**.

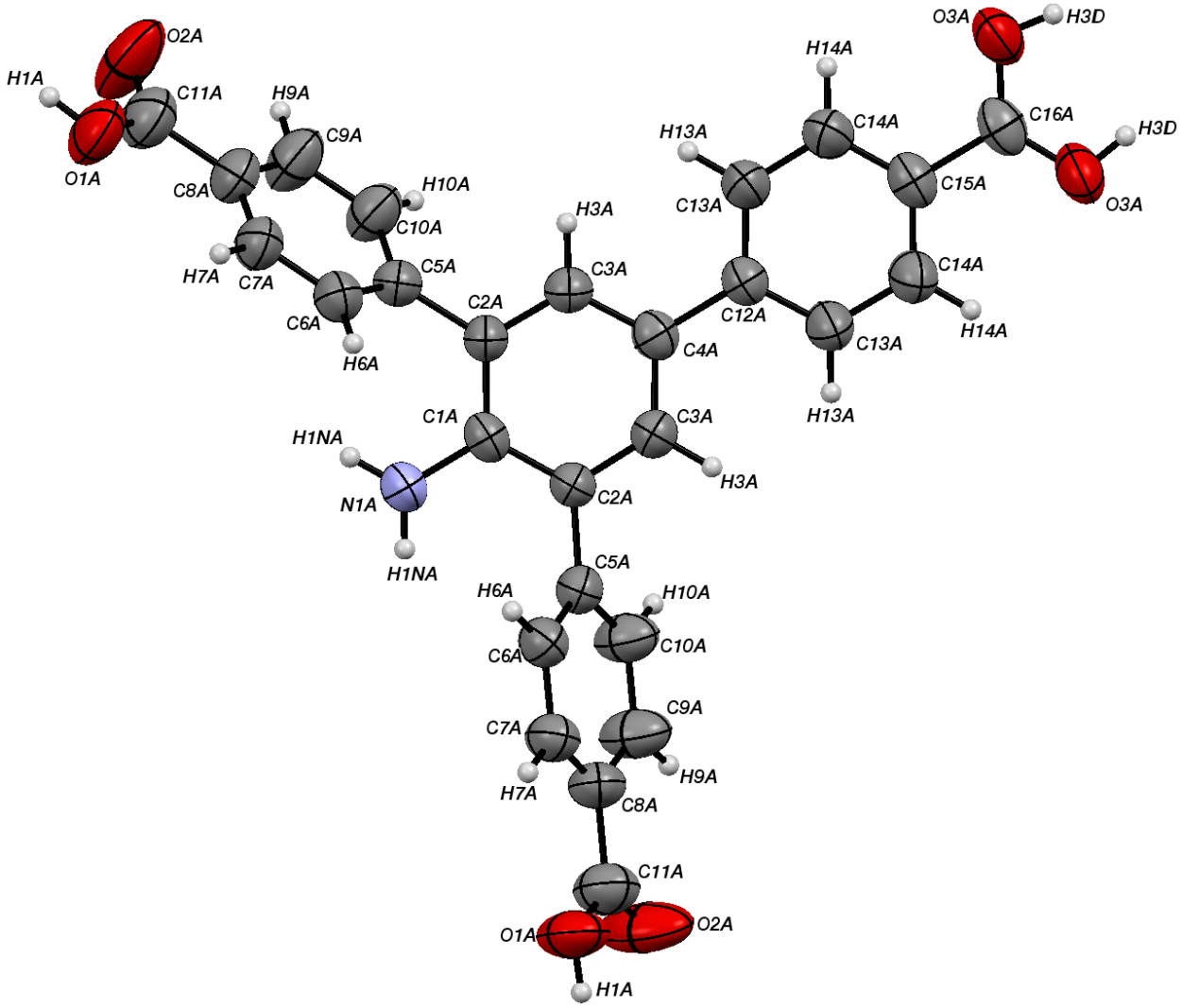

Figure S4a. ORTEP plot the first of the three crystallographically independent molecules in the asymmetric unit of compound **5**. All three crystallographically independent molecules are bisected by a mirror plane, inducing 1:1 disorder for the hydrogen atoms attached to O3A, O3B and O3C. Atoms created by the mirror plane carry non-capital labels a, b and c.

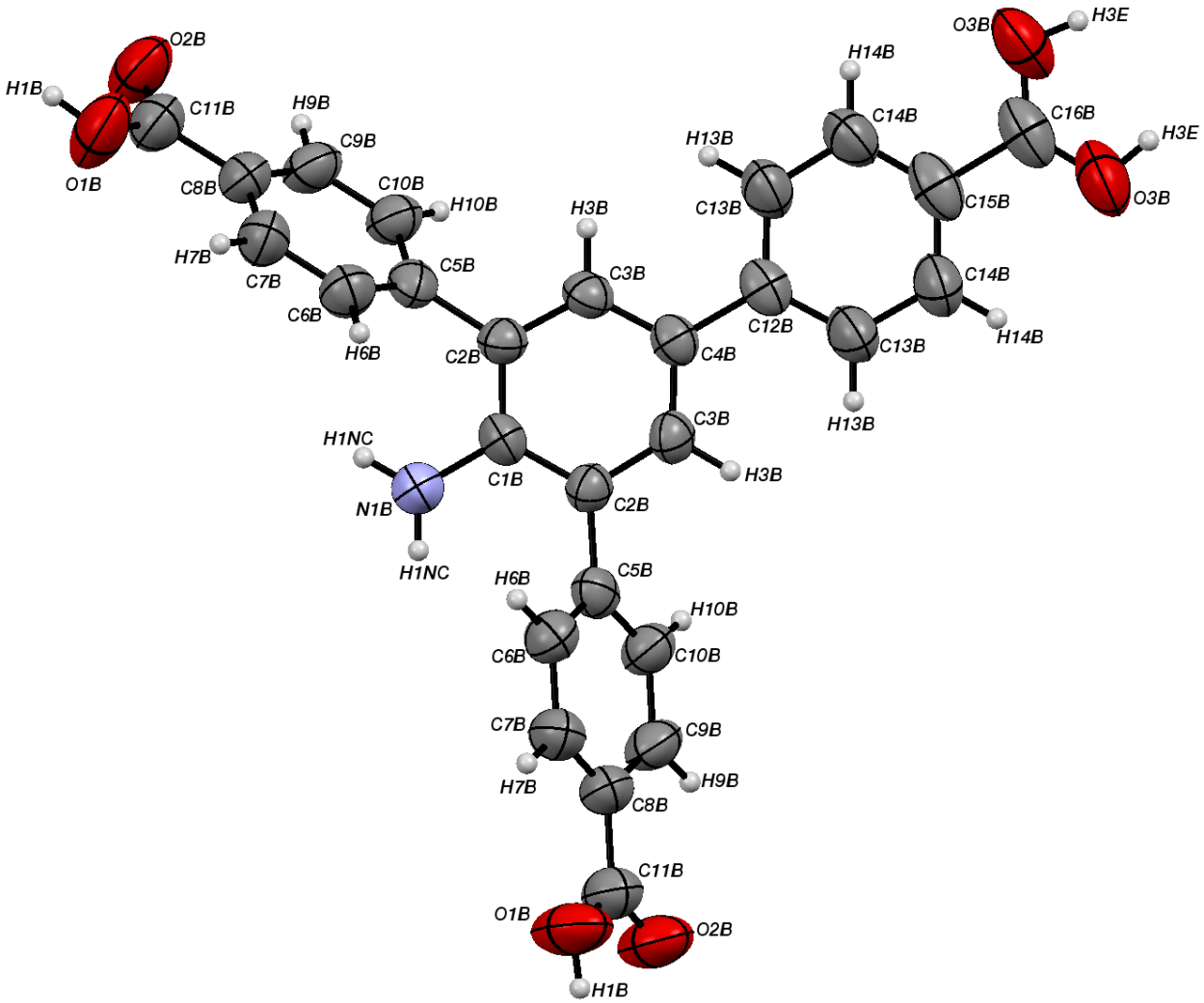

Figure S4b. ORTEP plot of the second of the three crystallographically independent molecules in the asymmetric unit of compound **5**. All three crystallographically independent molecules are bisected by a mirror plane, inducing 1:1 disorder for the hydrogen atoms attached to O3A, O3B and O3C. Atoms created by the mirror plane carry non-capital labels a, b and c.

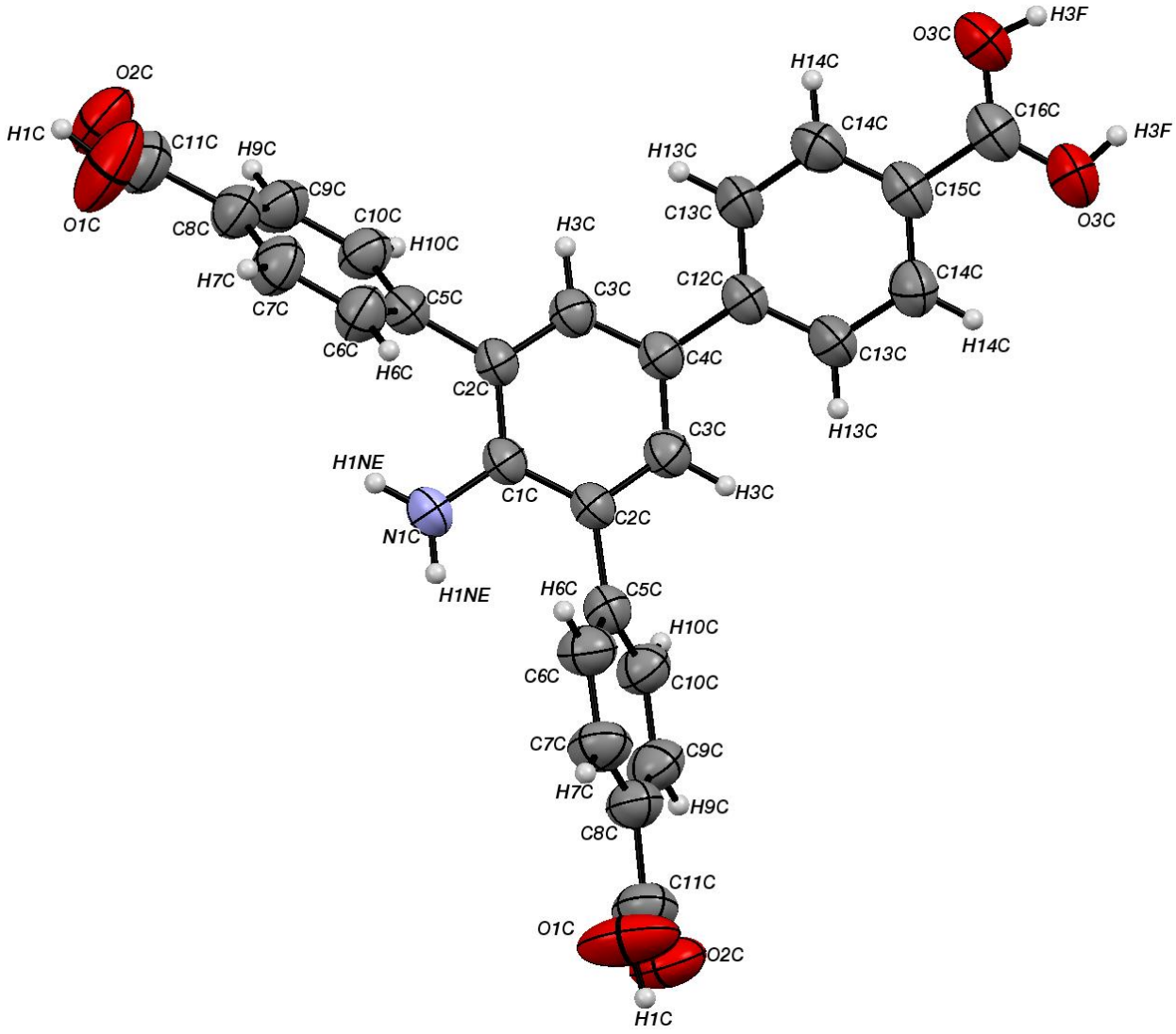

Figure S4c. ORTEP plot of the third of the three crystallographically independent molecules in the asymmetric unit of compound **5**. All three crystallographically independent molecules are bisected by a mirror plane, inducing 1:1 disorder for the hydrogen atoms attached to O3A, O3B and O3C. Atoms created by the mirror plane carry non-capital labels a, b and c.

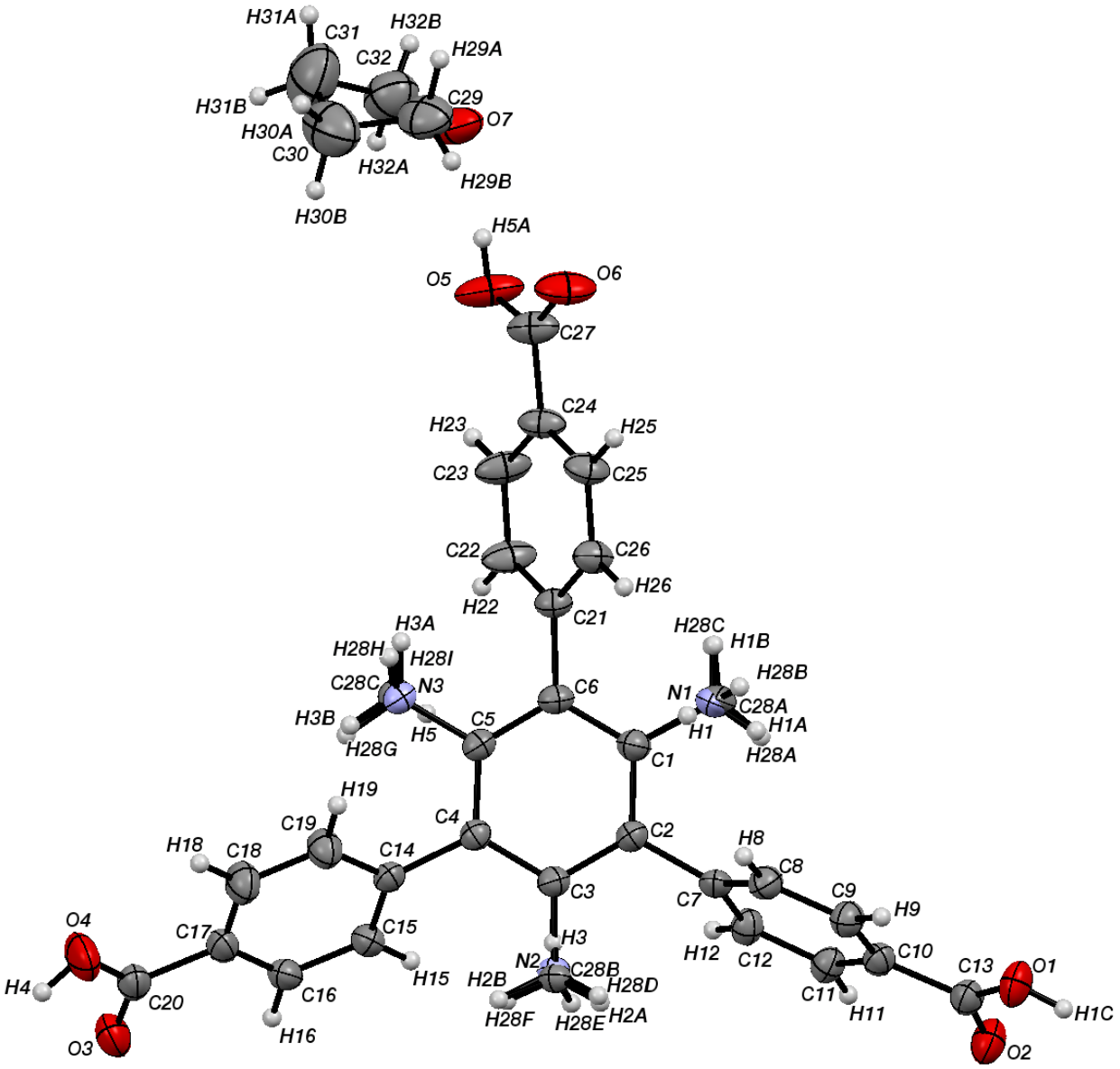

Figure S5. ORTEP plot of compound **6**. Methyl and amino groups are disordered (see SC-XRD Special Experimental Details).

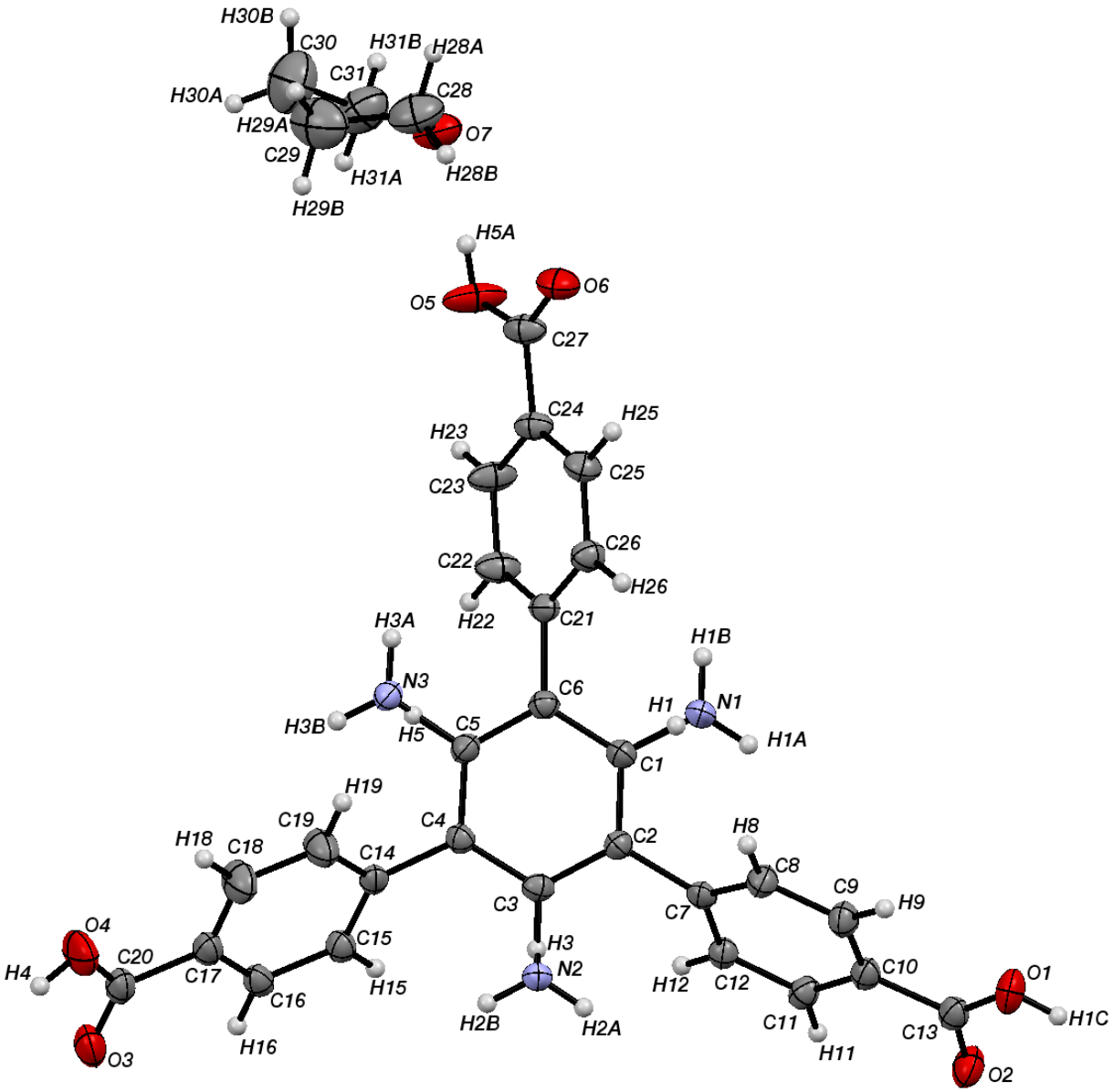

Figure S6. ORTEP plot of compound **7**. Amino groups are disordered (see SC-XRD Special Experimental Details).

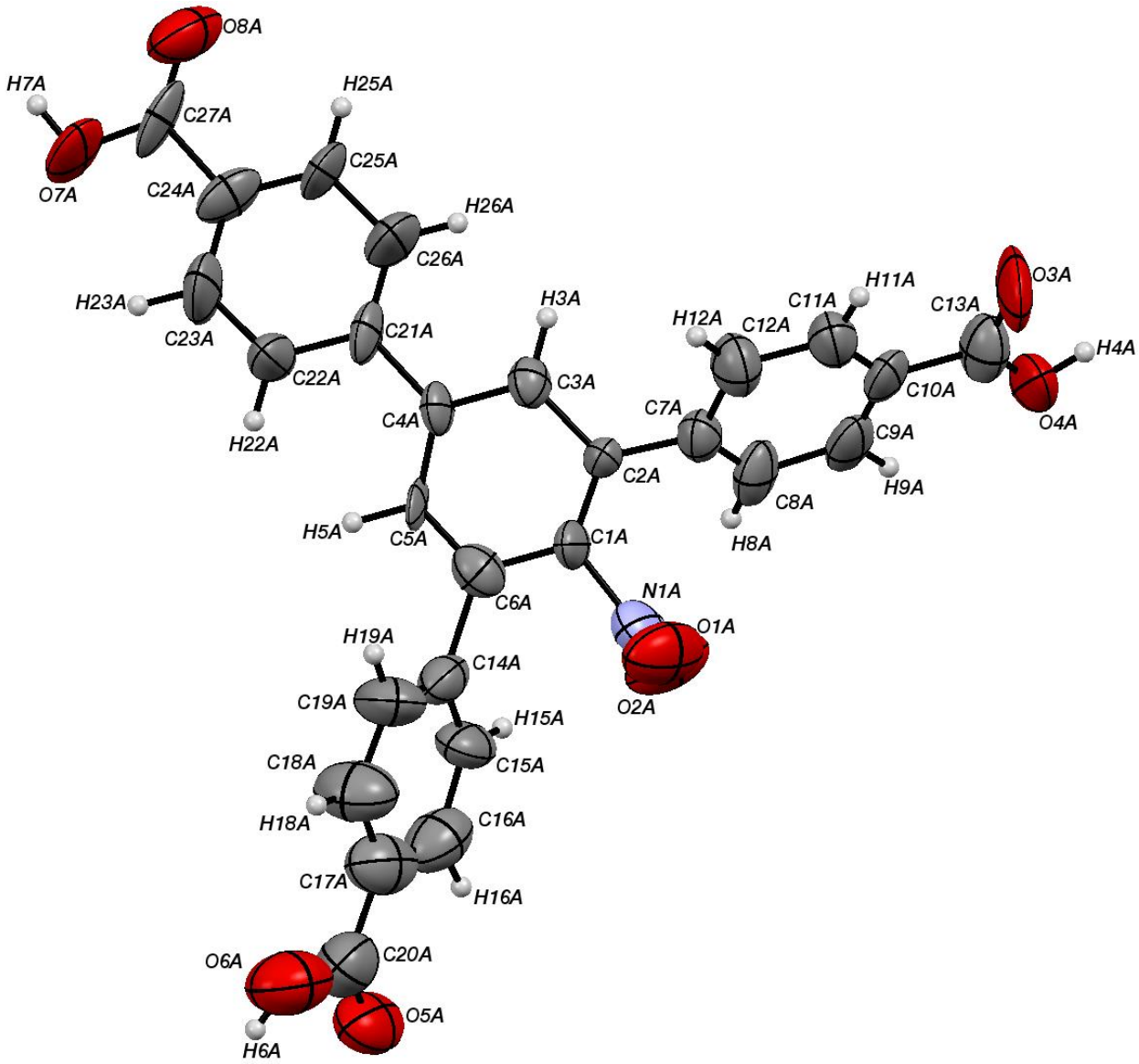

Figure S7a. ORTEP plot of the first of the two crystallographically independent molecules in the asymmetric unit of compound **8**.

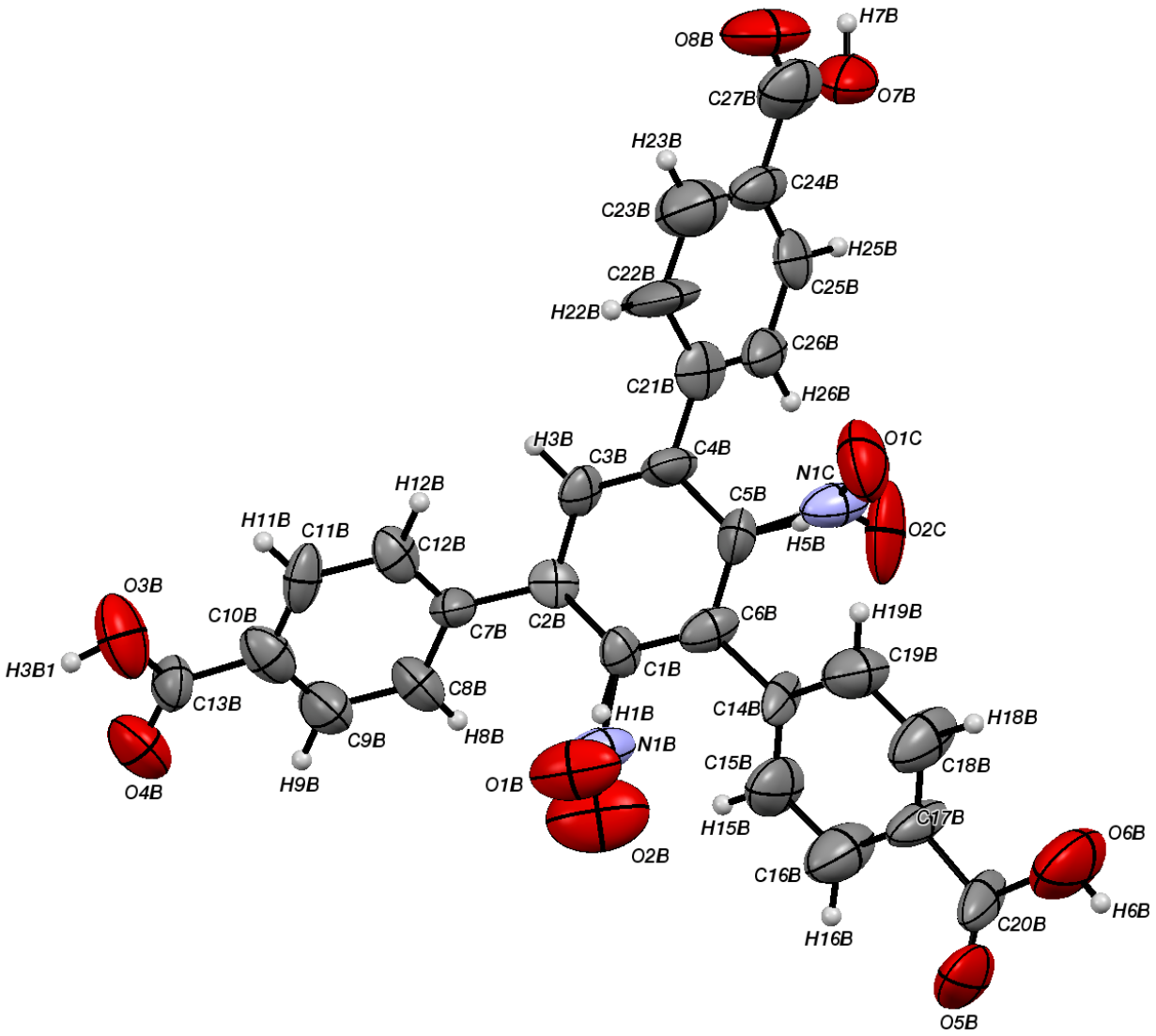

Figure S7b. ORTEP plot of the second of the two crystallographically independent molecules in the asymmetric unit of compound **8**. The nitro group on this molecule is disordered (see SC-XRD Special Experimental Details).

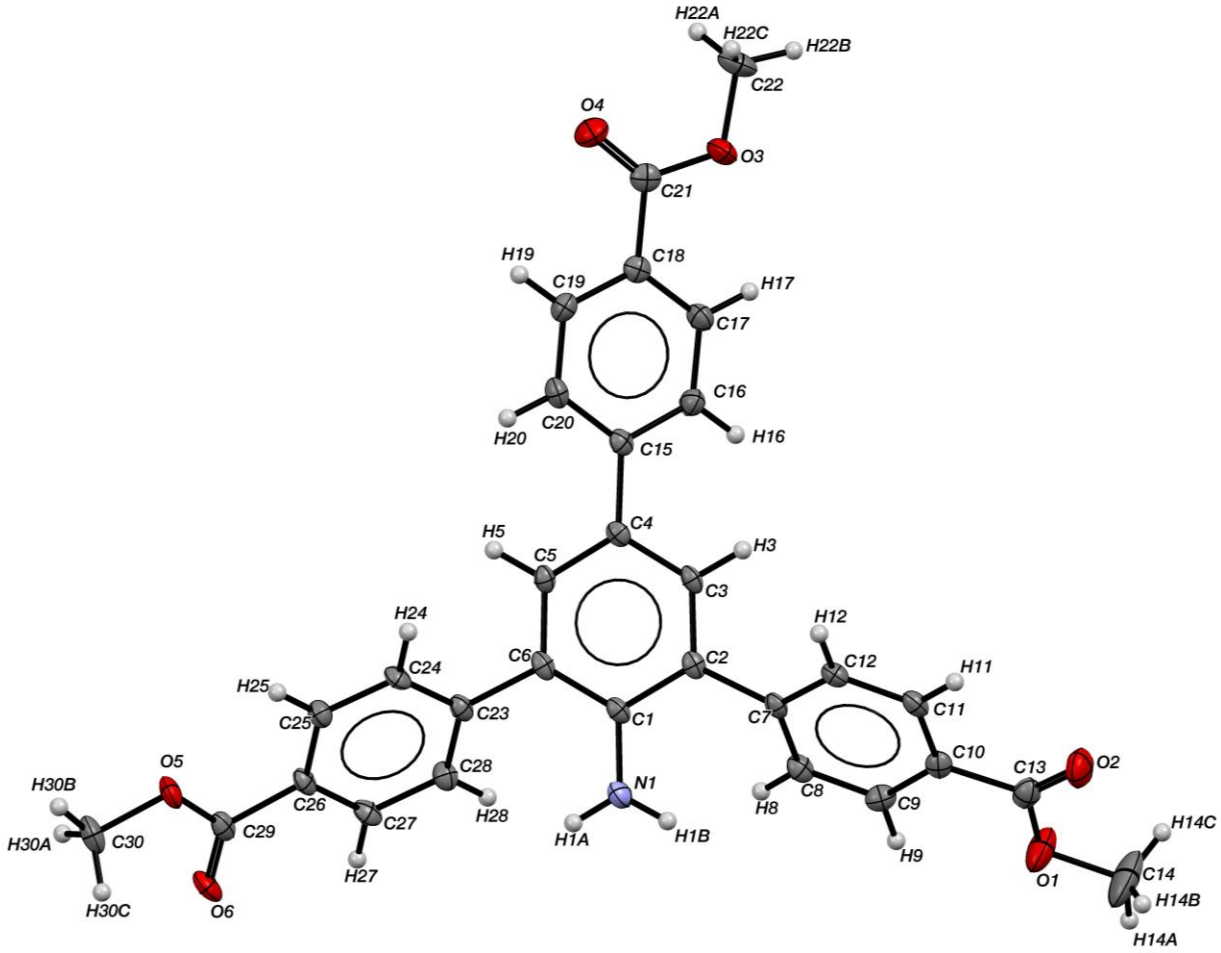

Figure S8. ORTEP plot of 2,4,6-tris(4-carboxyphenyl)aniline trimethyl ester, synthetic intermediate of **5**.

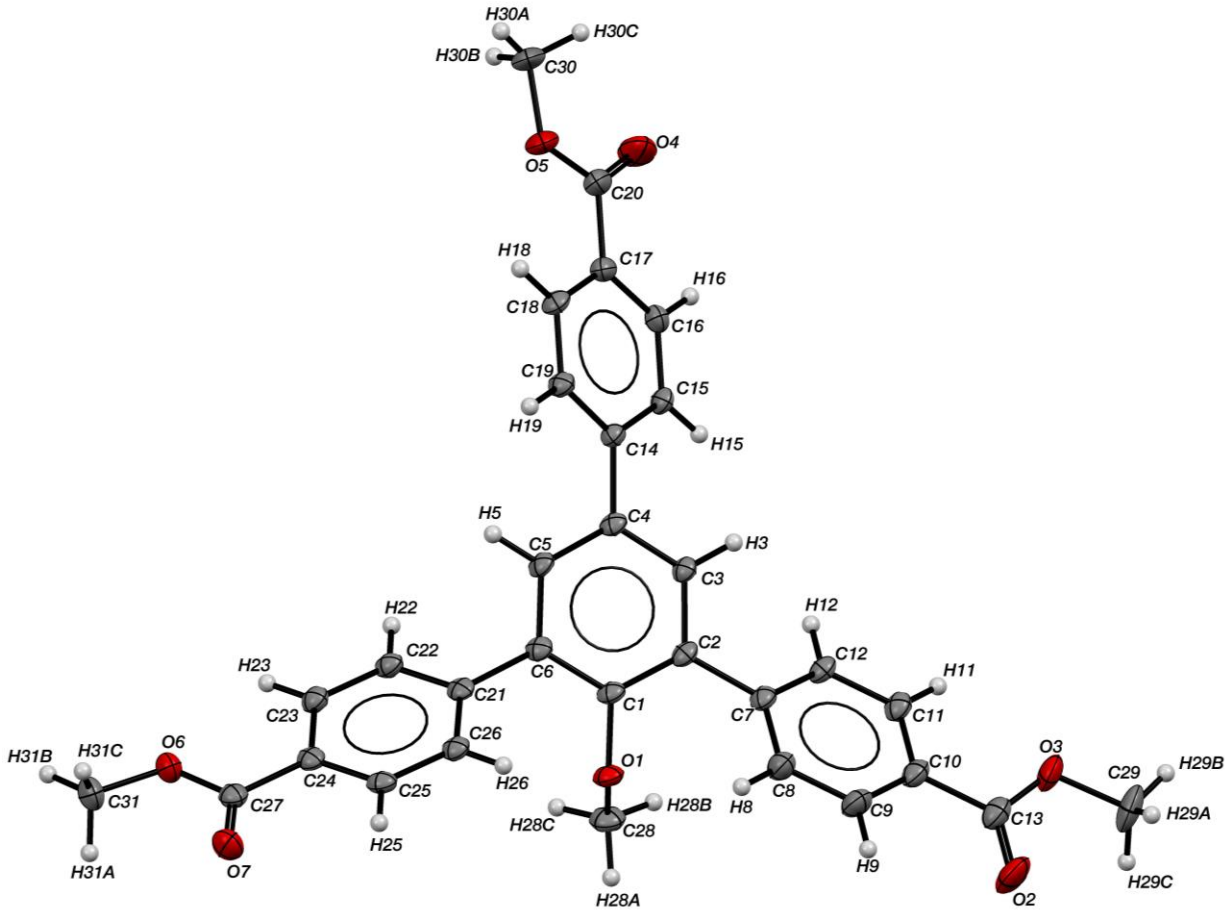

Figure S9. ORTEP plot of 2,4,6-tris(4-carboxyphenyl)anisole trimethyl ester, synthetic intermediate of **3**.

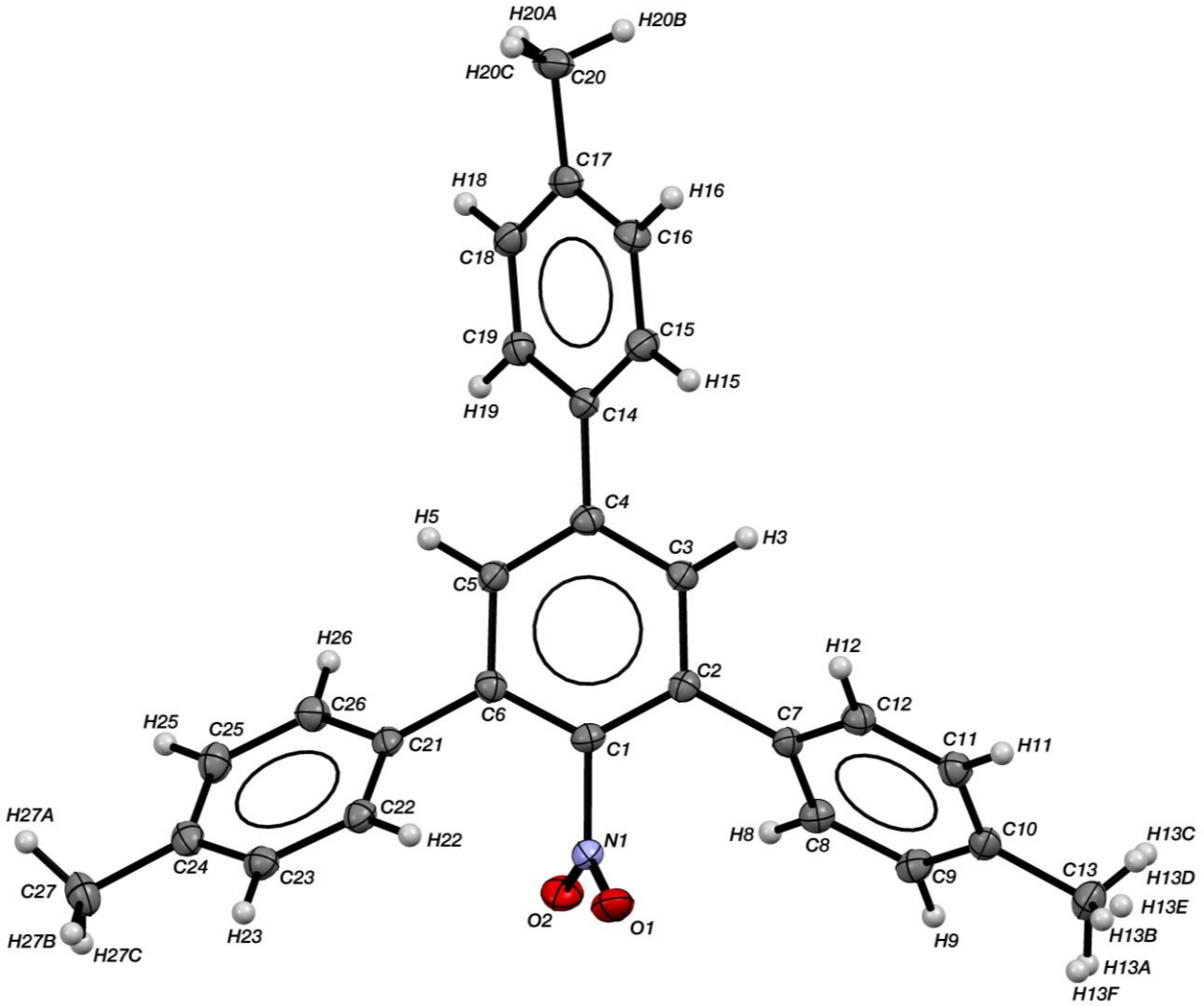

Figure S10. ORTEP plot of tritolylnitrobenzene, synthetic intermediate of **8**.

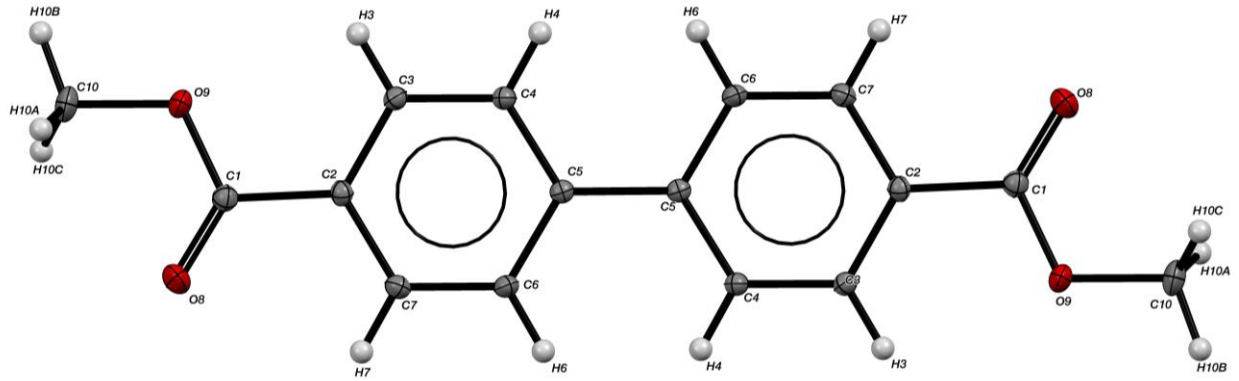

Figure S11. ORTEP plot of dimethyl biphenyl-4,4'-dicarboxylate, homo-coupling product from Suzuki reactions. The molecule is located on a crystallographic inversion center.

Diffraction Images

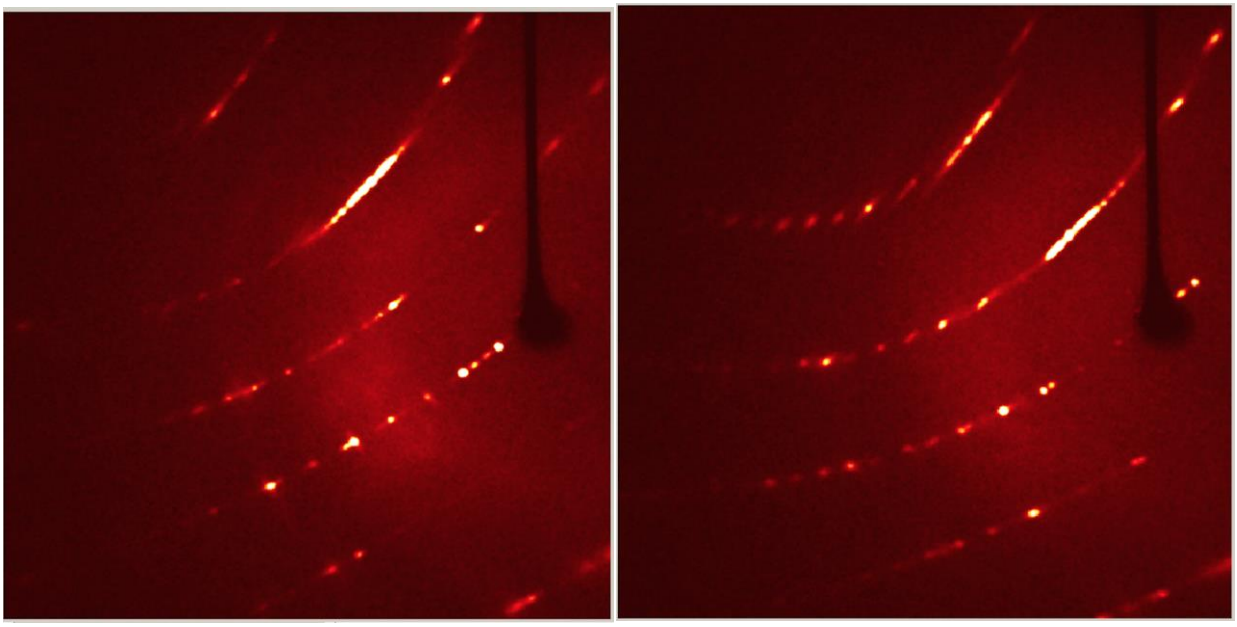

Figure S12. Diffraction images of **6** grown by vapor diffusion using solvent/antisolvent pair 1,4-dioxane/acetonitrile. Notice the excessive non-Bragg behavior as evident from the streaking of diffracted intensity between Bragg peaks.

Experimental and Calculated PXRD Diffractograms

A Rigaku Ultima IV diffractometer (λ = 1.5418 Å) with Bragg Brentano geometry was used for the following room temperature PXRD experiments. A scan speed of 4 degrees/minute was used. PXRD experiments were performed in open atmosphere after the crystals were filtered off and allowed to air dry over a glass frit.

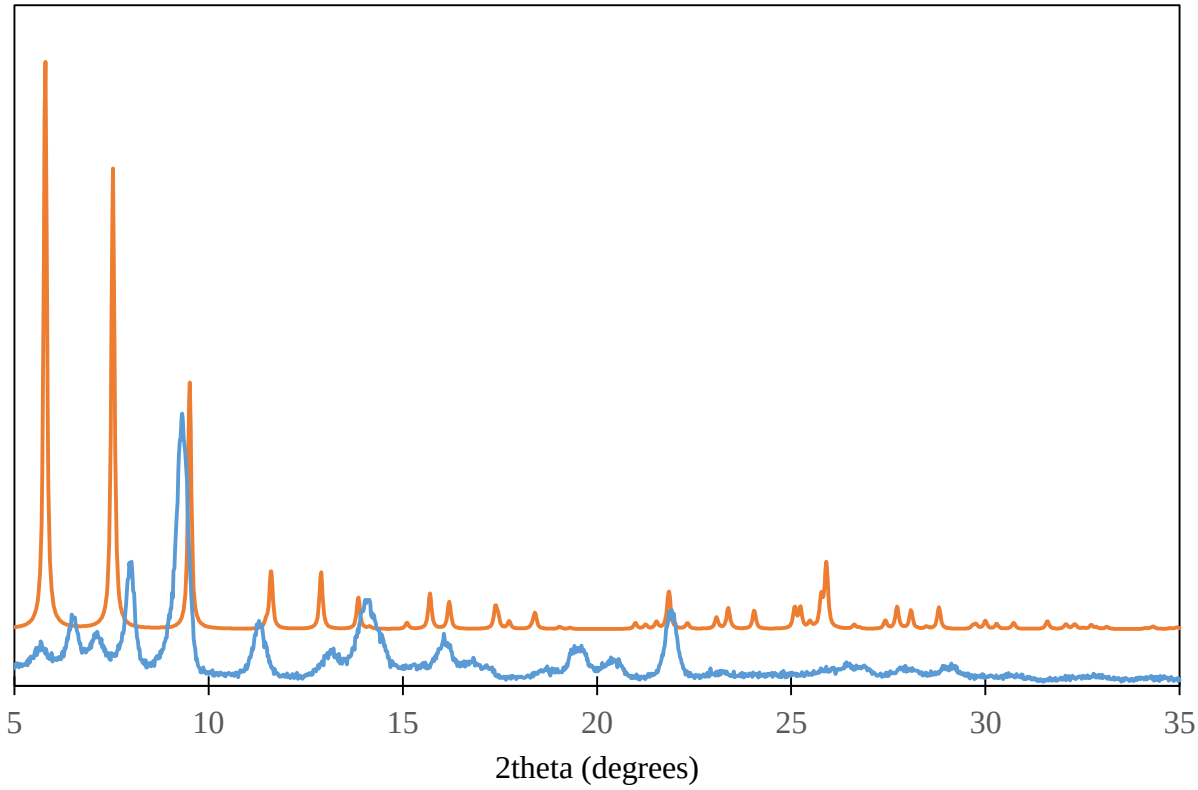

Figure S13. PXRD diffractogram of **2** calculated from the SC-XRD experiment (orange) and XRD pattern measured after removal of crystals from solvent (blue).

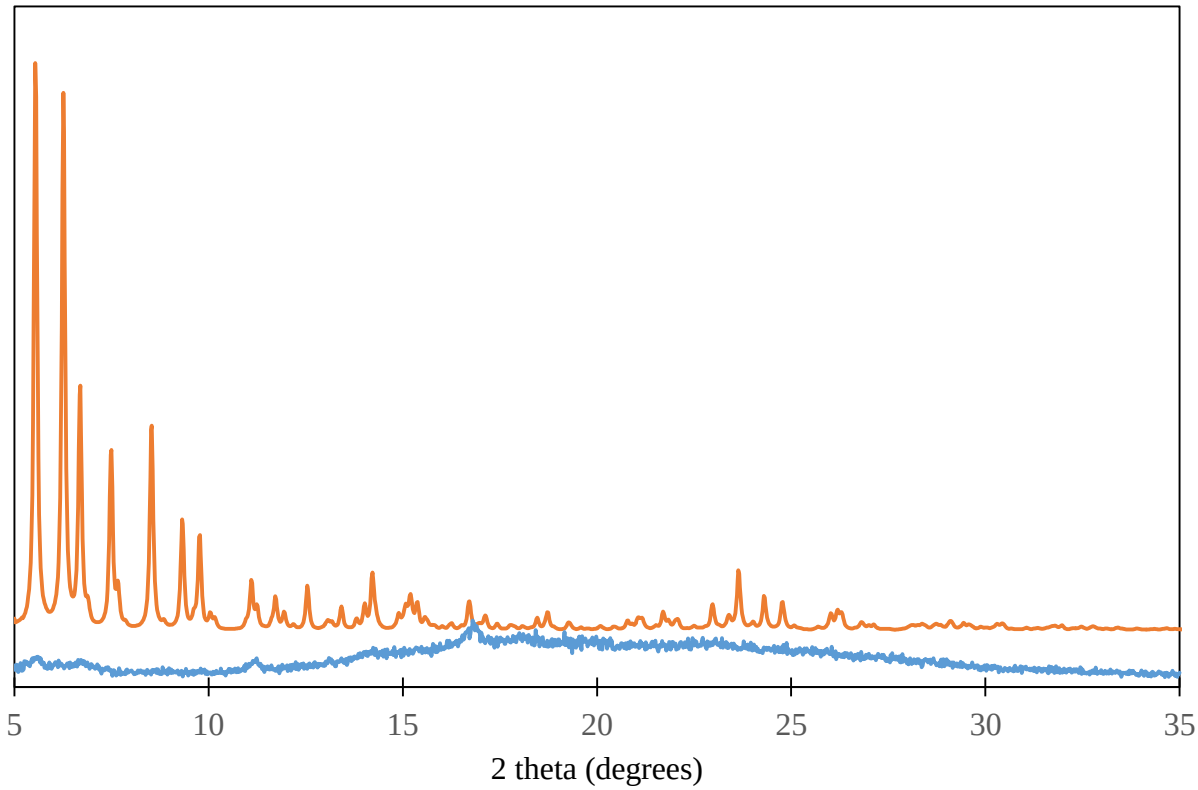

Figure S14. PXRD diffractogram of **3** calculated from the SC-XRD experiment (orange) and measured after removal of crystals from solvent (blue).

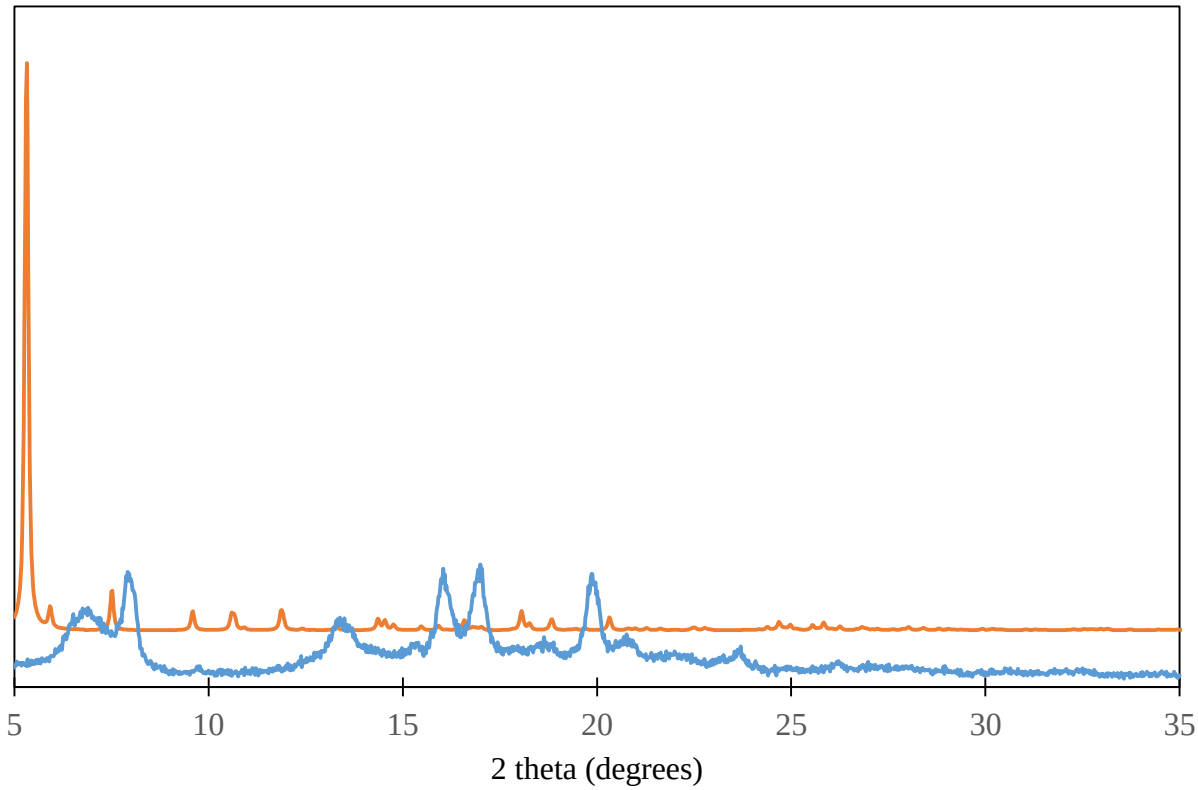

Figure S15. PXRD diffractogram of **4** calculated from the SC-XRD experiment (orange) and measured after removal of crystals from solvent (blue).

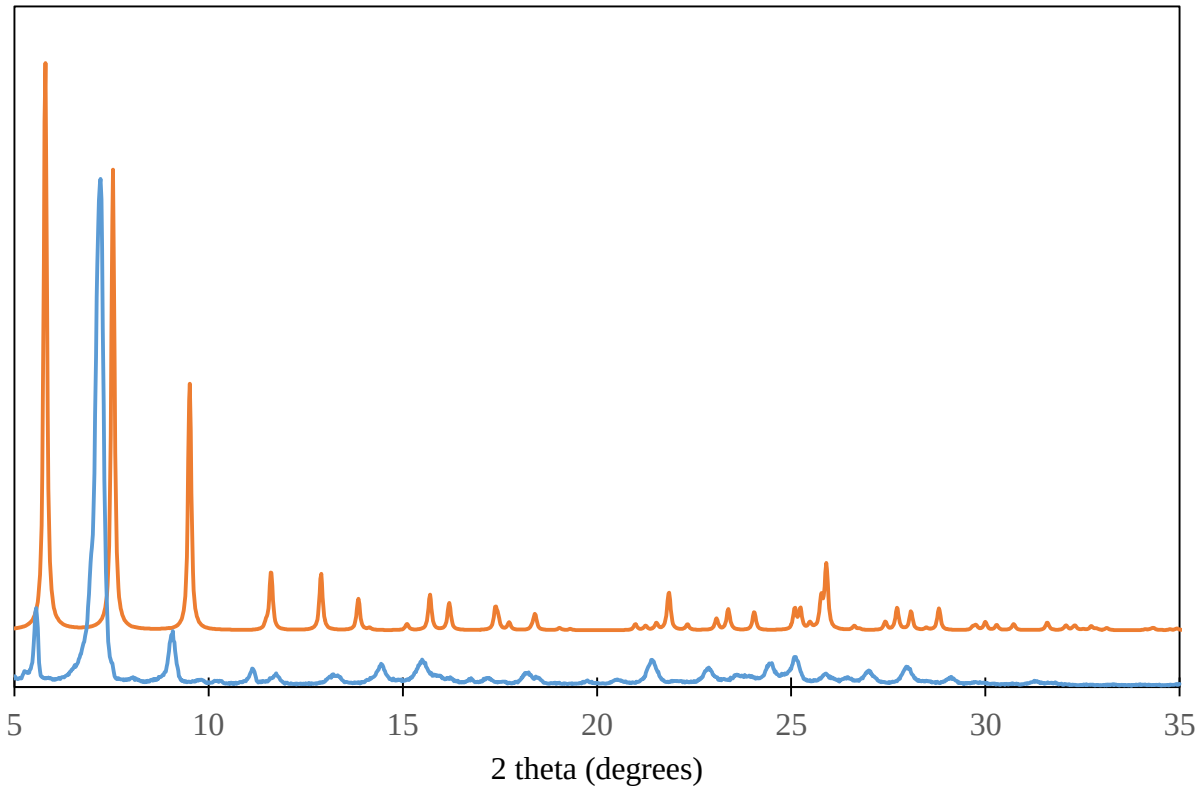

Figure S16. PXRD diffractogram of the crystals of **5** calculated from the SC-XRD experiment (orange) and measured after removal of crystals from solvent (blue). Comparison of the patterns indicates a substantial expansion and slight change of the framework lattice upon warming up from 100 K (SC data) to room temperature (experimental pattern), but no fundamental change of the overall structure.

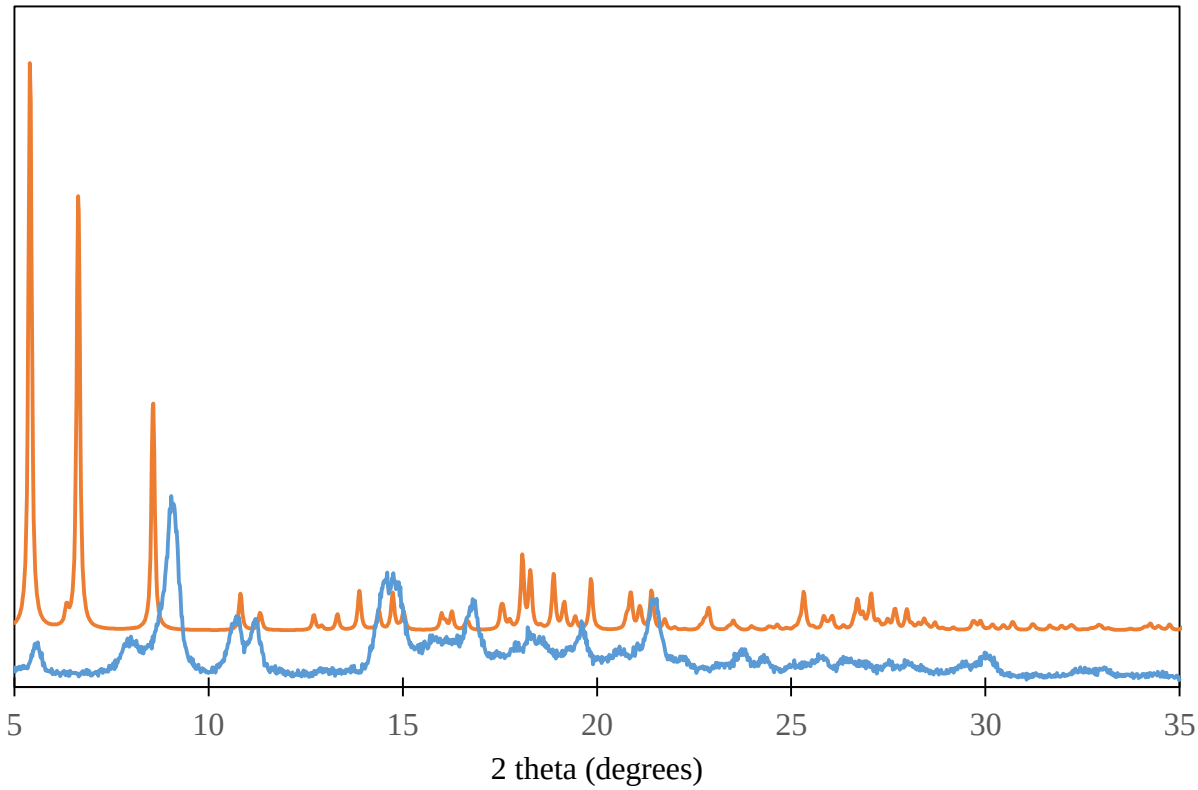

Figure S17. PXRD diffractogram of the crystals of **6** calculated from the SC-XRD experiment (orange) and measured after removal of crystals from solvent (blue).

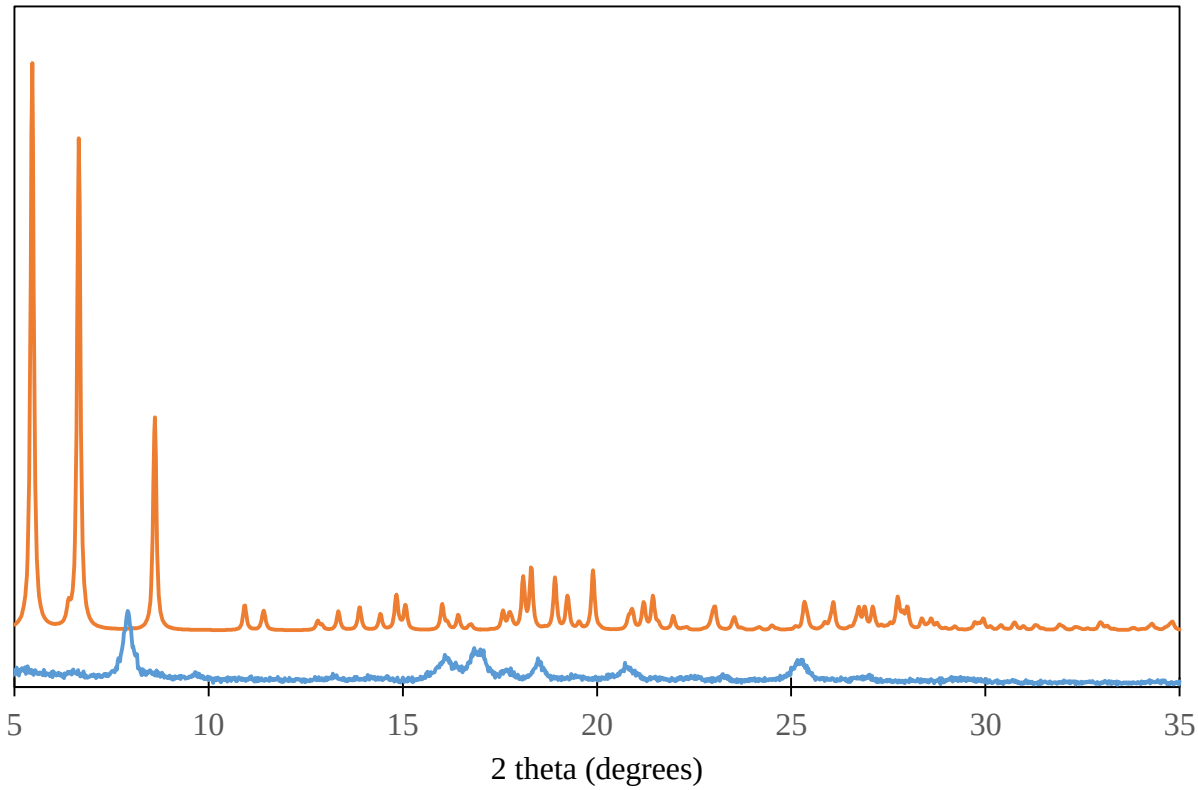

Figure S18. PXRD diffractogram of **7** calculated from the SC-XRD experiment (orange) and measured after removal of crystals from solvent (blue).

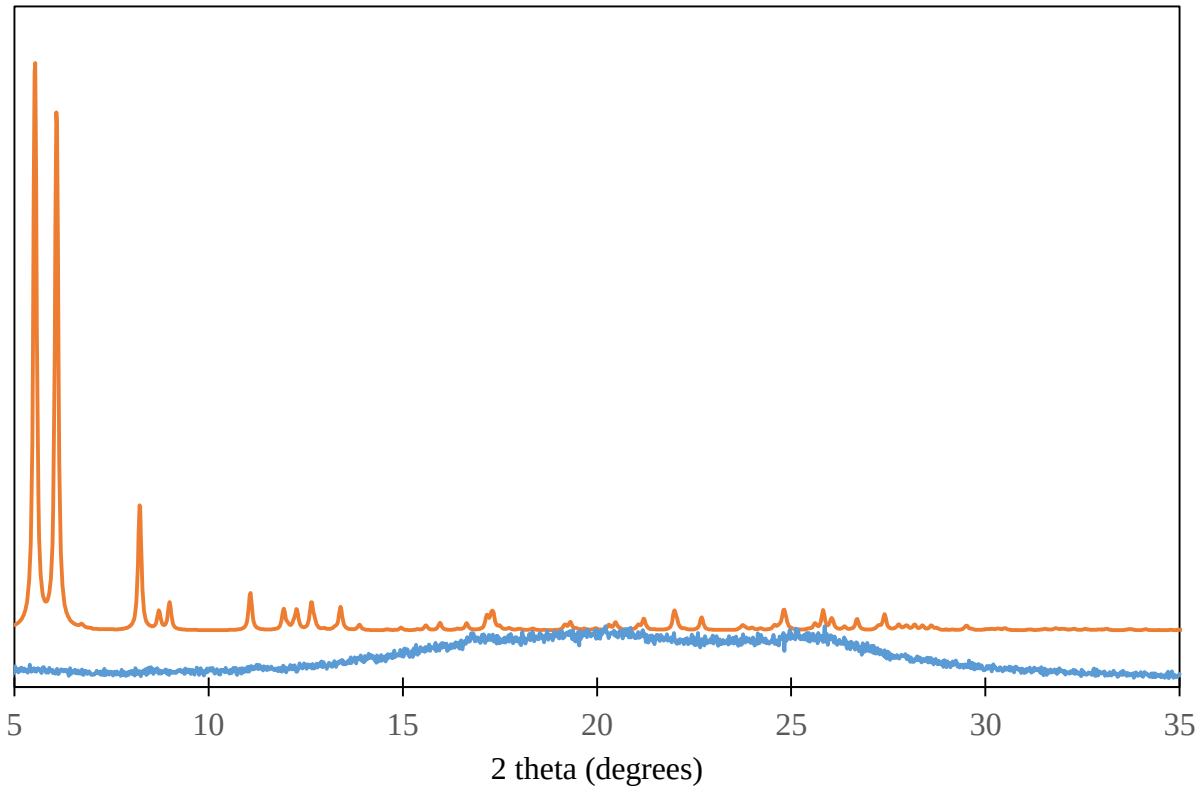

Figure S19. PXRD diffractogram of **8** calculated from the SC-XRD experiment (orange) and measured after removal of crystals from solvent (blue).

Thermal Gravimetric Analysis and Differential Scanning Calorimetry

Thermal gravimetric analyses and differential scanning calorimetry were performed simultaneously on a Mettler Toledo TGA/DSC 1 STAR^{e} System. Experiments were performed under nitrogen after the crystals were filtered and allowed to air dry over a glass frit. Temperature was raised at 2 °C/min.

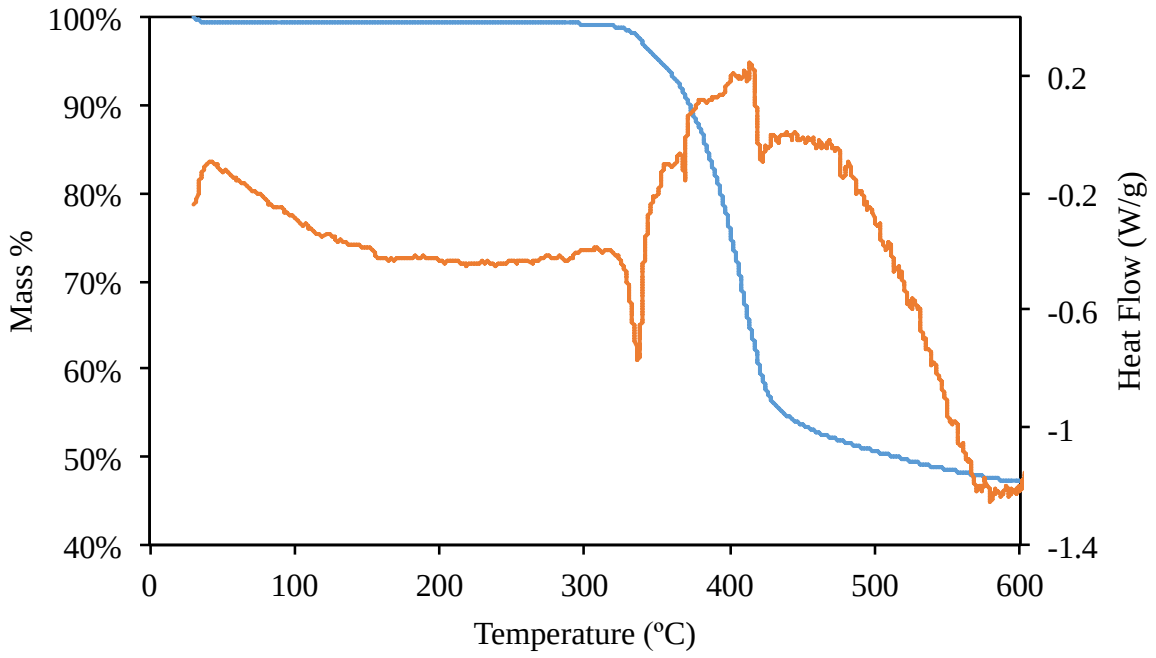

Figure S20. TGA (blue) and DSC (orange) traces of of the crystals of **2**.

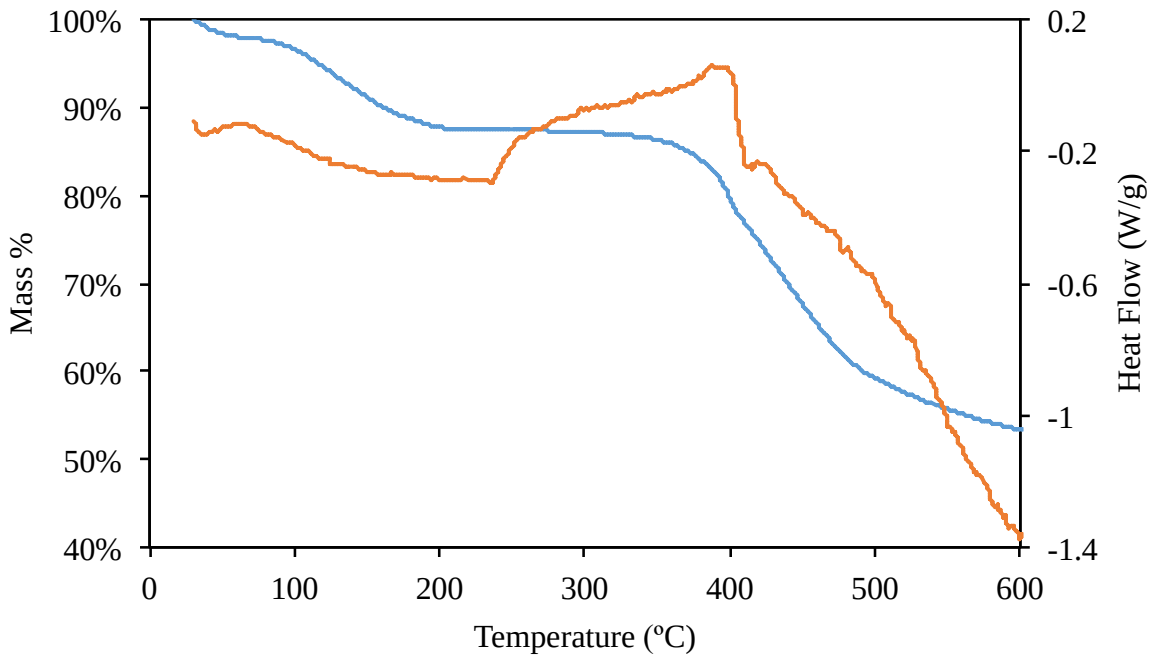

Figure S21. TGA (blue) and DSC (orange) traces of of the crystals of **3**.

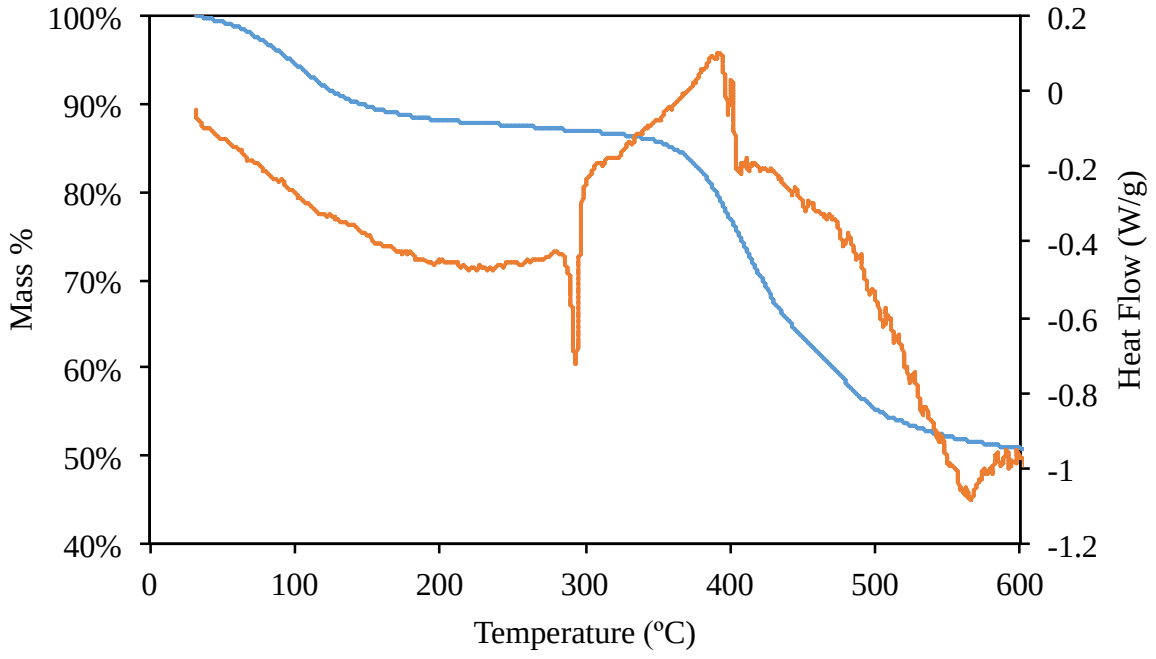

Figure S22. TGA (blue) and DSC (orange) traces of of the crystals of **4**.

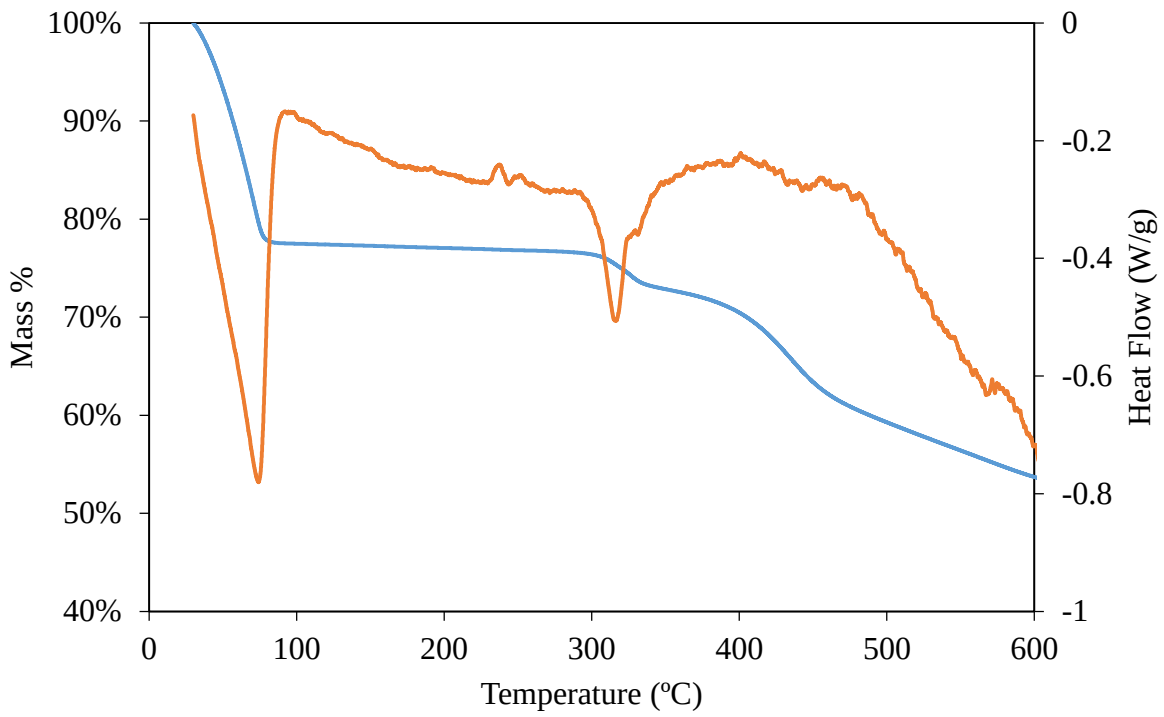

Figure S23. TGA (blue) and DSC (orange) traces of of the crystals of **5**.

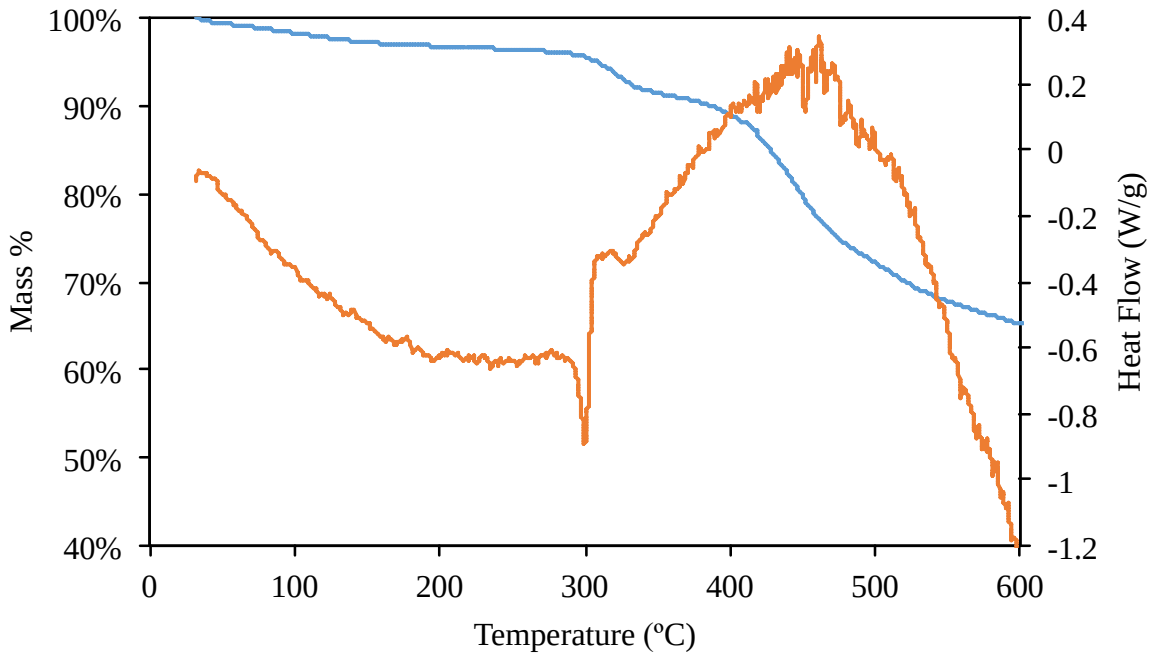

Figure S24. TGA (blue) and DSC (orange) traces of of the crystals of **6.**

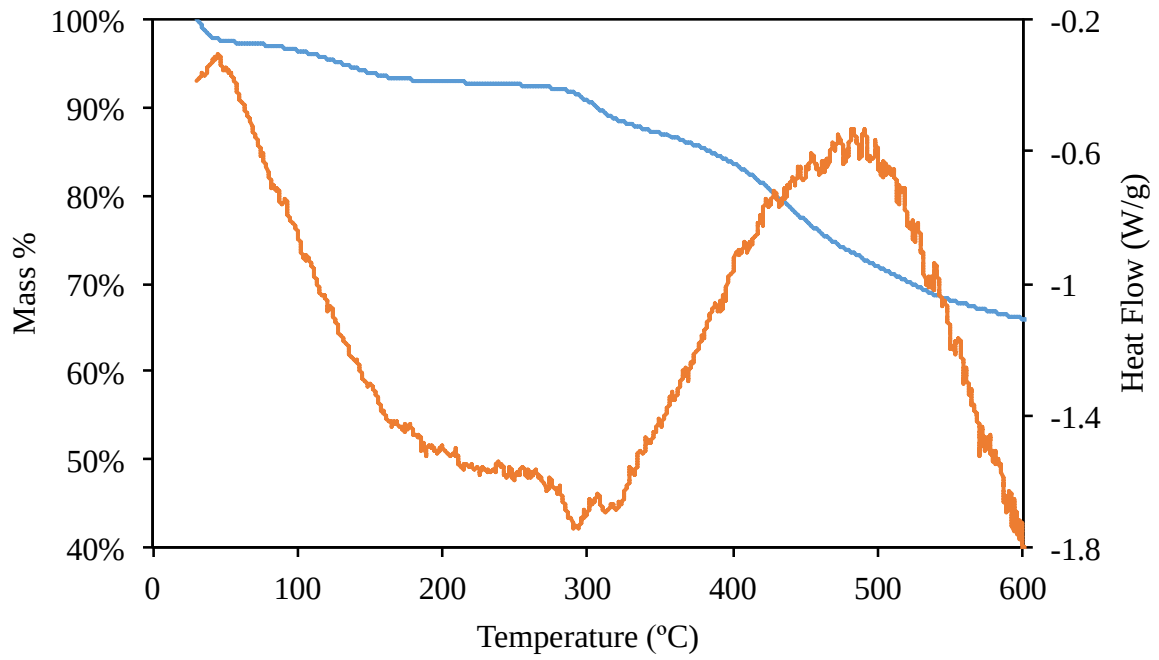

Figure S25. TGA (blue) and DSC (orange) traces of of the crystals of **7**.

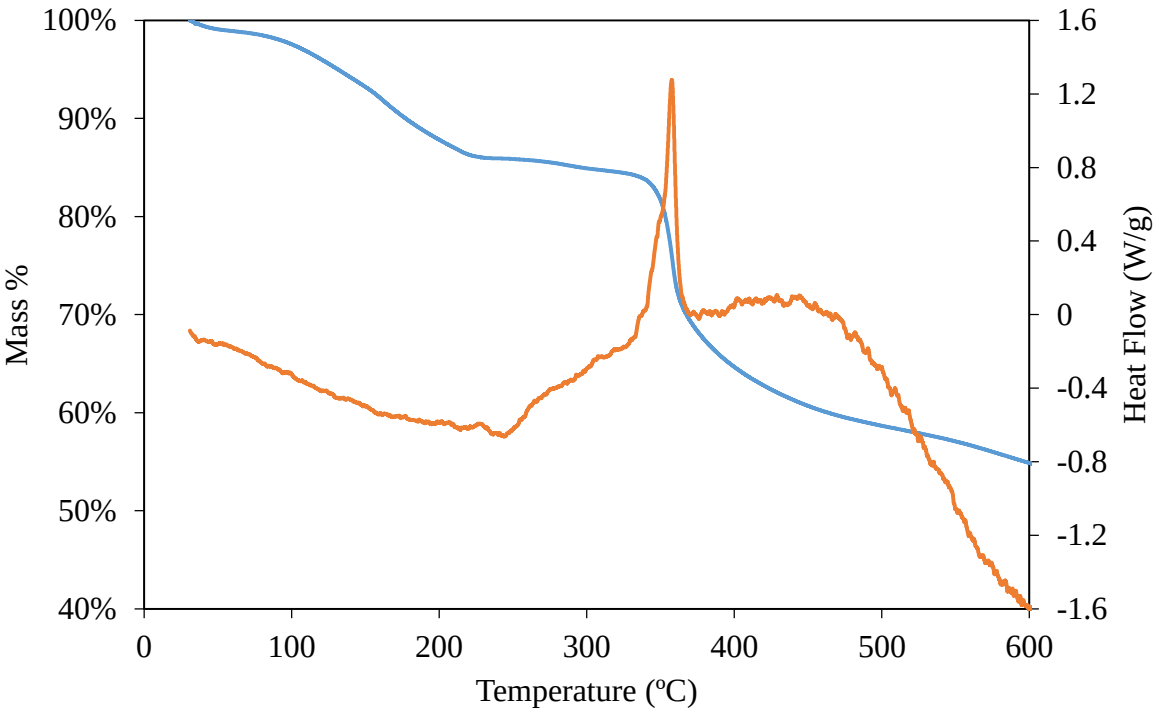

Figure S26. TGA (blue) and DSC (orange) traces of of the crystals of **8**.

^{1}H and ^{13}C NMR Experiments

A Varian 400 MHz NMR spectrometer was used. All NMR spectra were taken at room temperature with spinning at 20 Hz. Shimming and locking were performed using the Varian VnmrJ software. Crystals were dissolved in DMSO-d_6 after they were filtered and allowed to air dry over a glass frit.

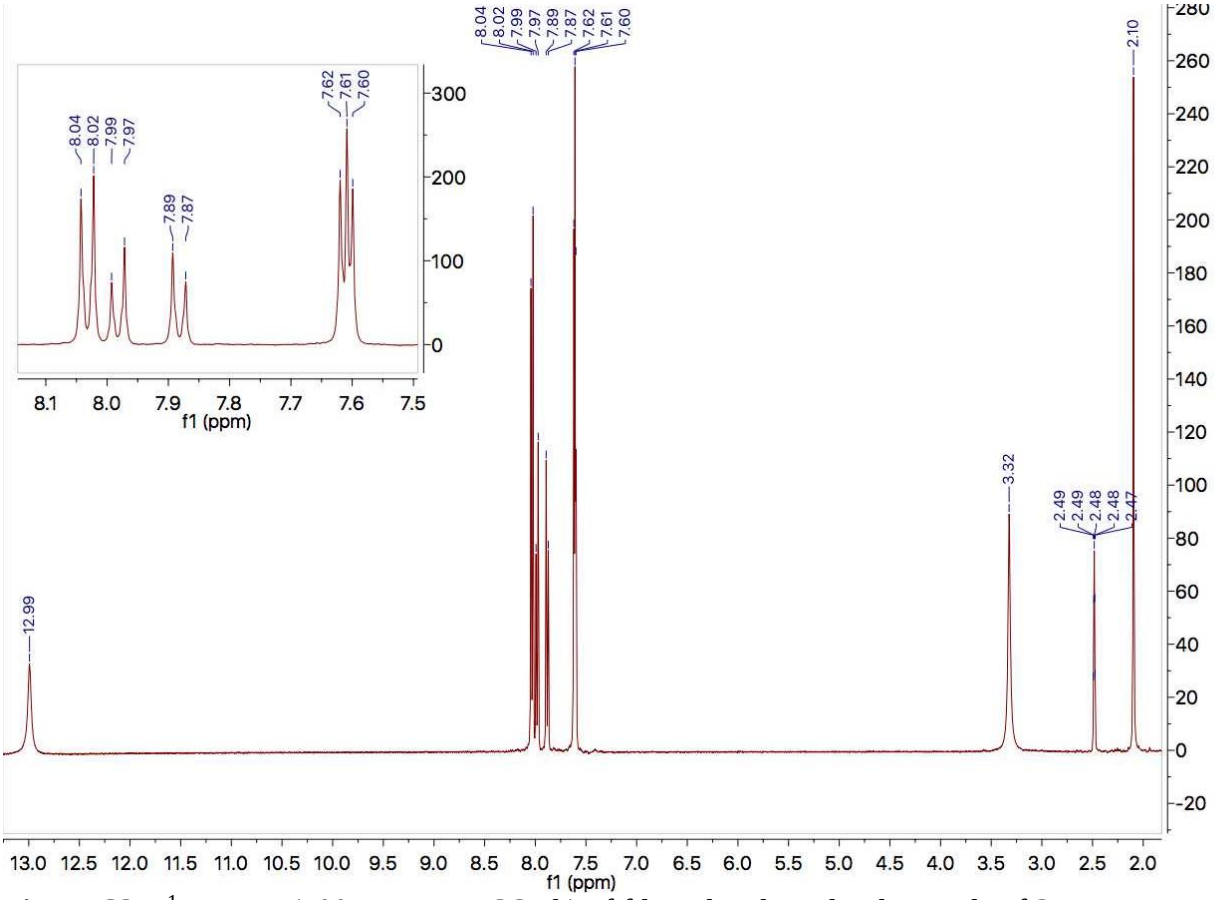

Figure S27. ^{1}H NMR (400 MHz, DMSO-d_6) of filtered and air-dried crystals of **2**.

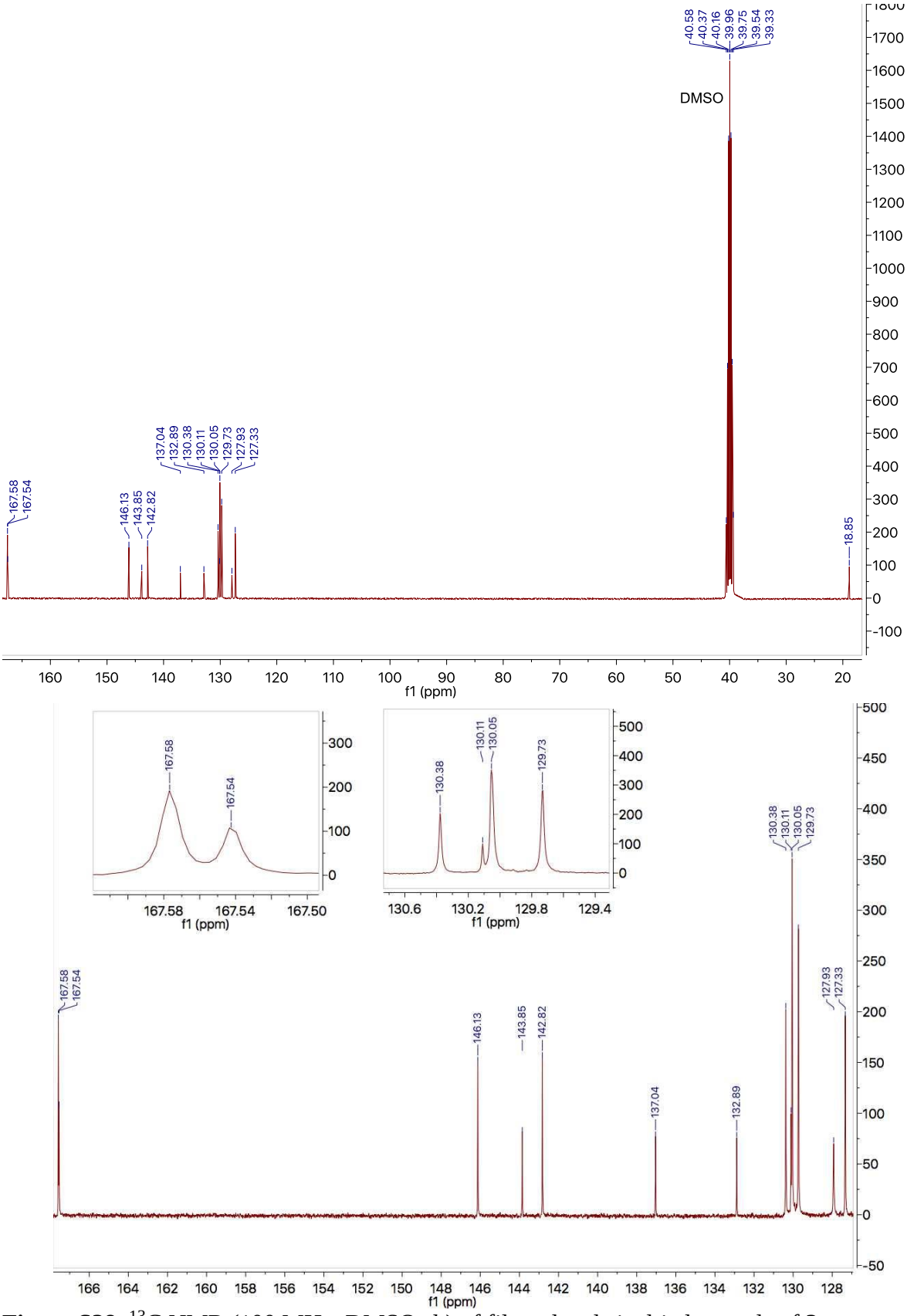

Figure S28. ^{13}C NMR (100 MHz, DMSO-d_6) of filtered and air-dried crystals of **2**.

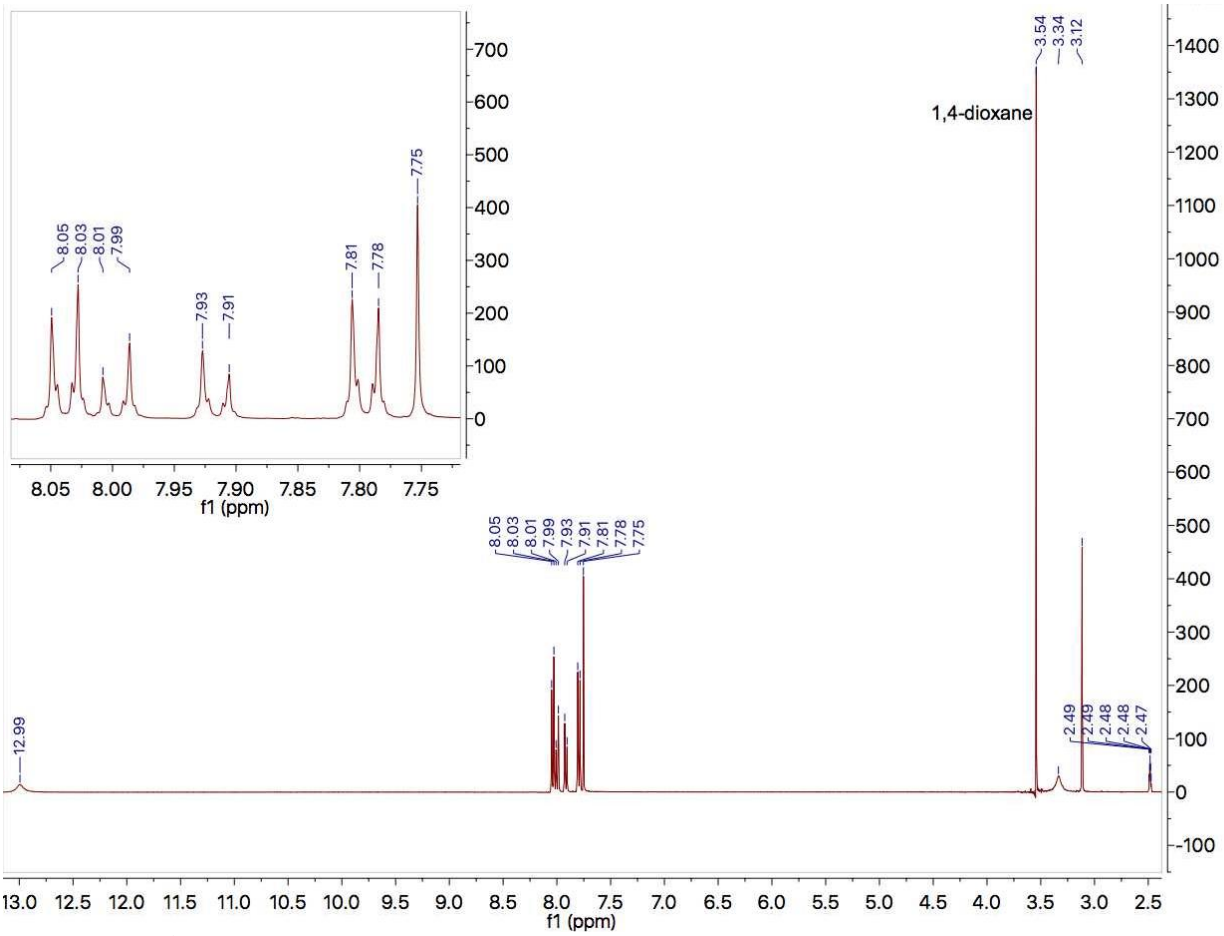

Figure S29. ^{1}H NMR (400 MHz, DMSO-d_6) of filtered and air-dried crystals of **3**.

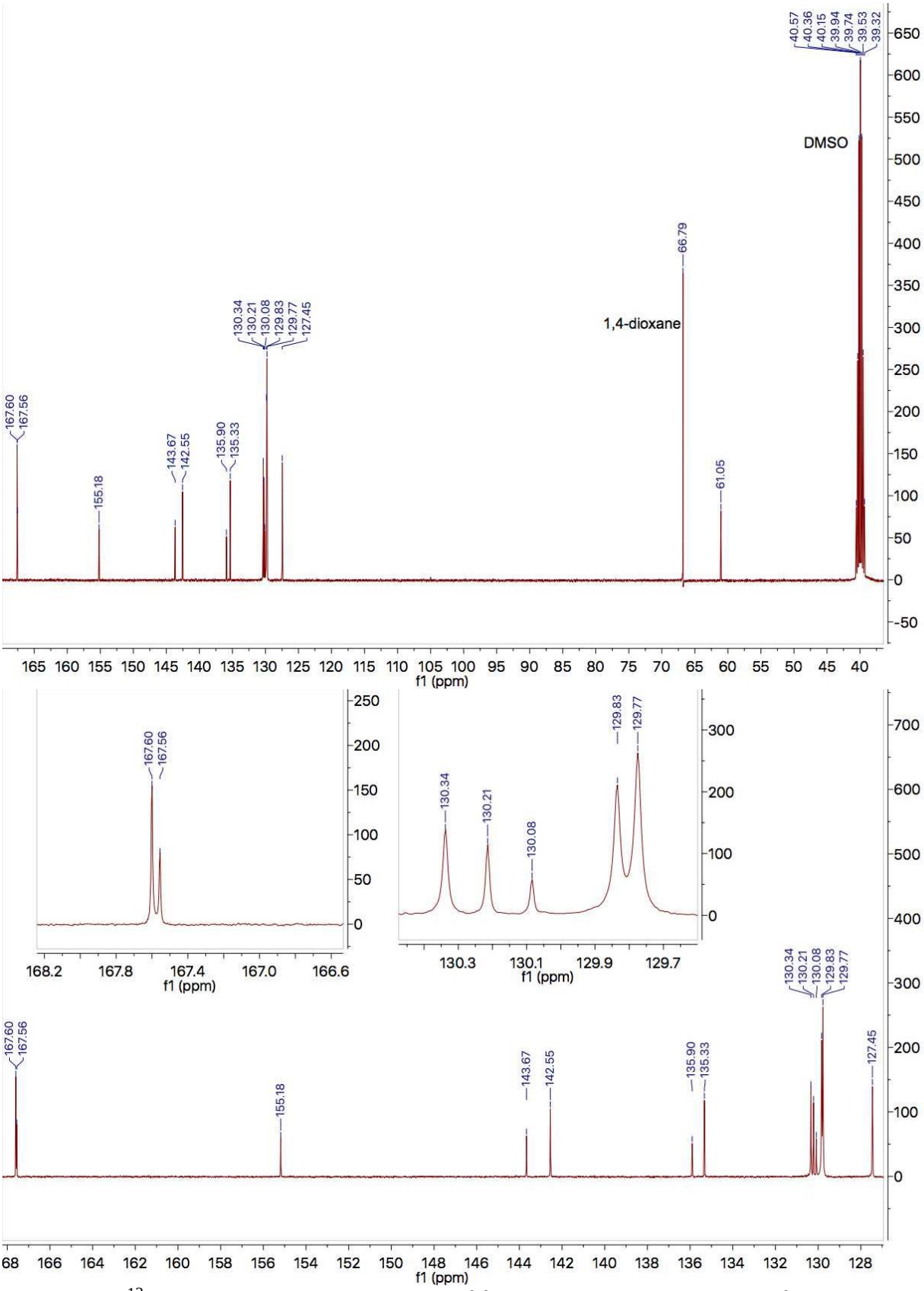

Figure S30. ^{13}C NMR (100 MHz, DMSO-d_6) of filtered and air-dried crystals of **3**.

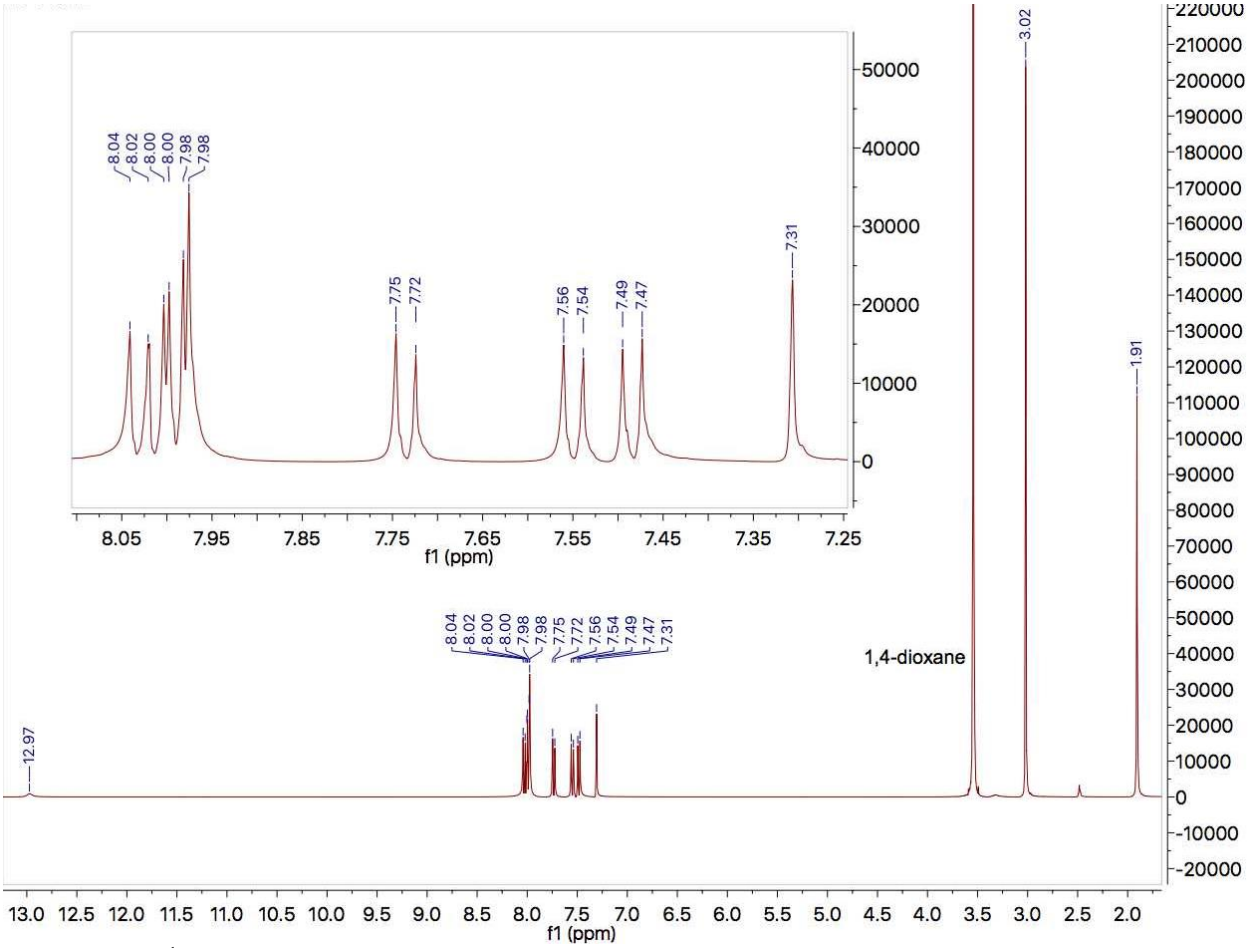

Figure S31. ^{1}H NMR (400 MHz, DMSO-d_6) of filtered and air-dried crystals of **4**.

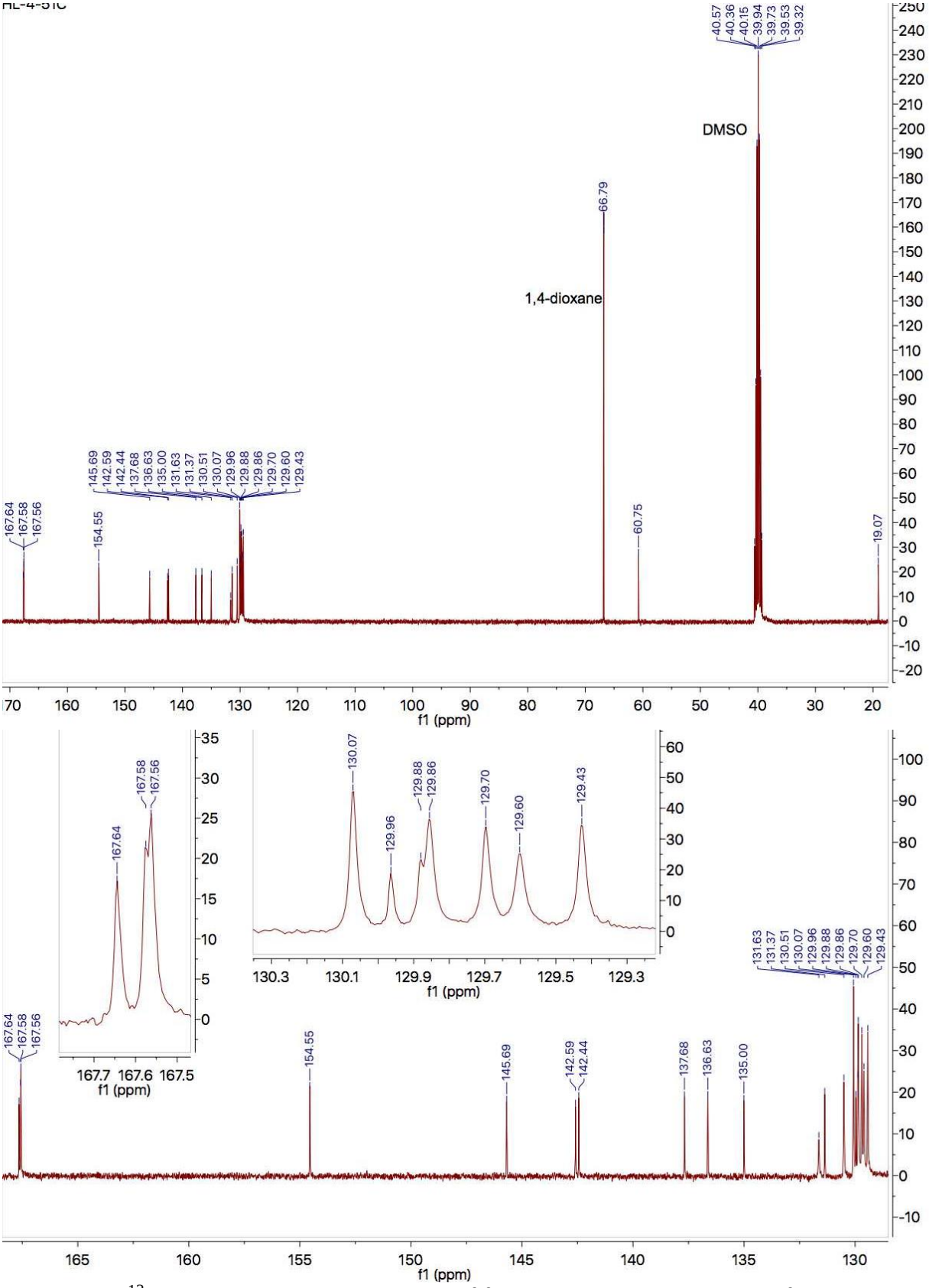

Figure S32. ^{13}C NMR (100 MHz, DMSO-d_6) of filtered and air-dried crystals of **4**.

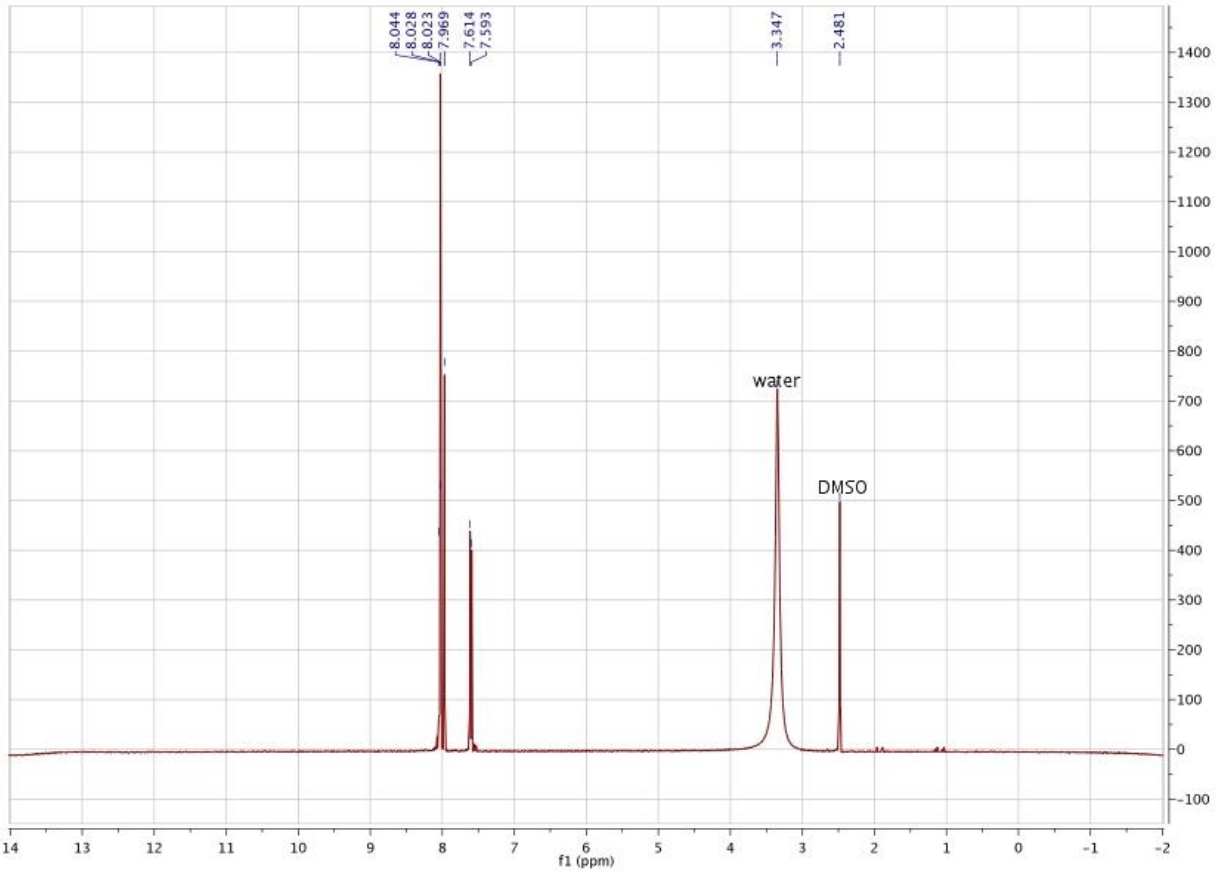

Figure S33. ^{1}H NMR (400 MHz, DMSO-d_6) of filtered and air-dried crystals of **5**.

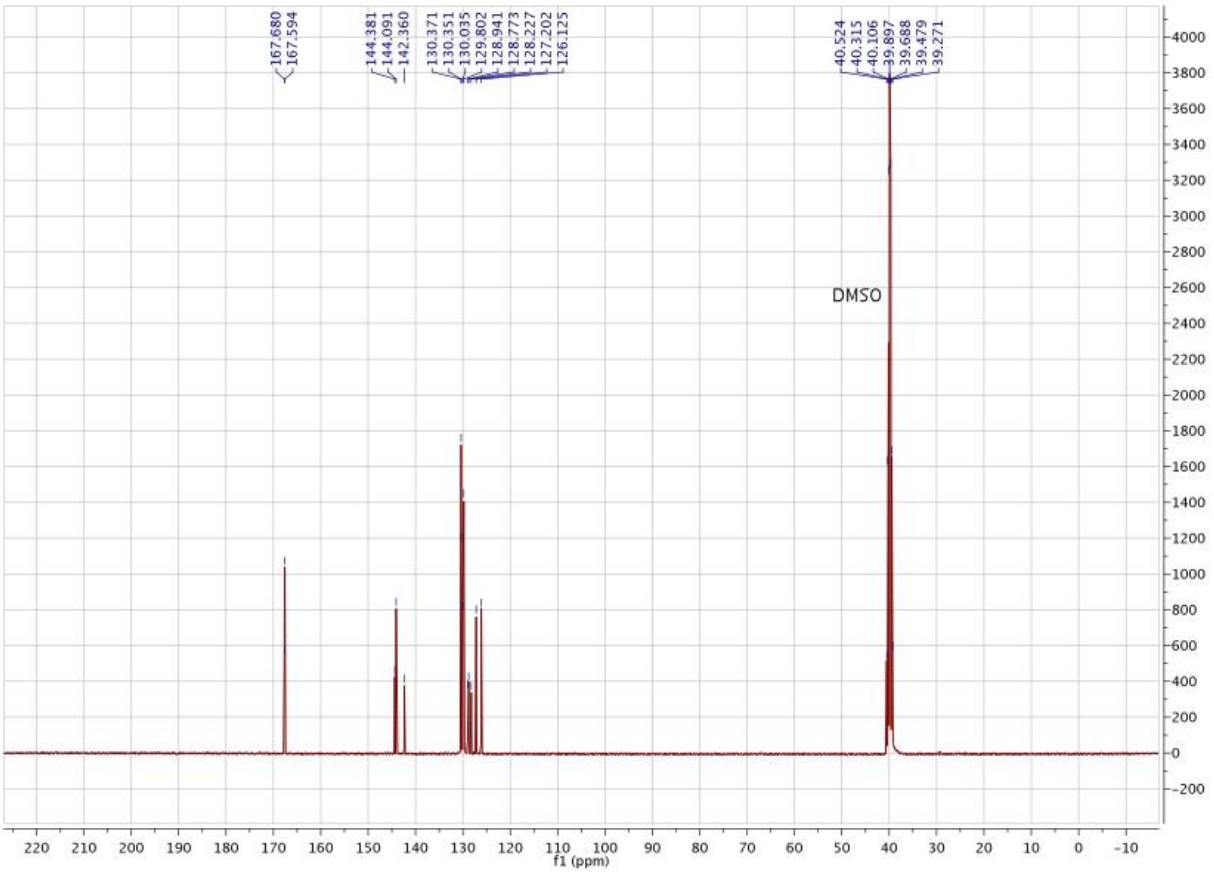

Figure S34. ^{13}C NMR (100 MHz, DMSO-d_6) of filtered and air-dried crystals of **5**.

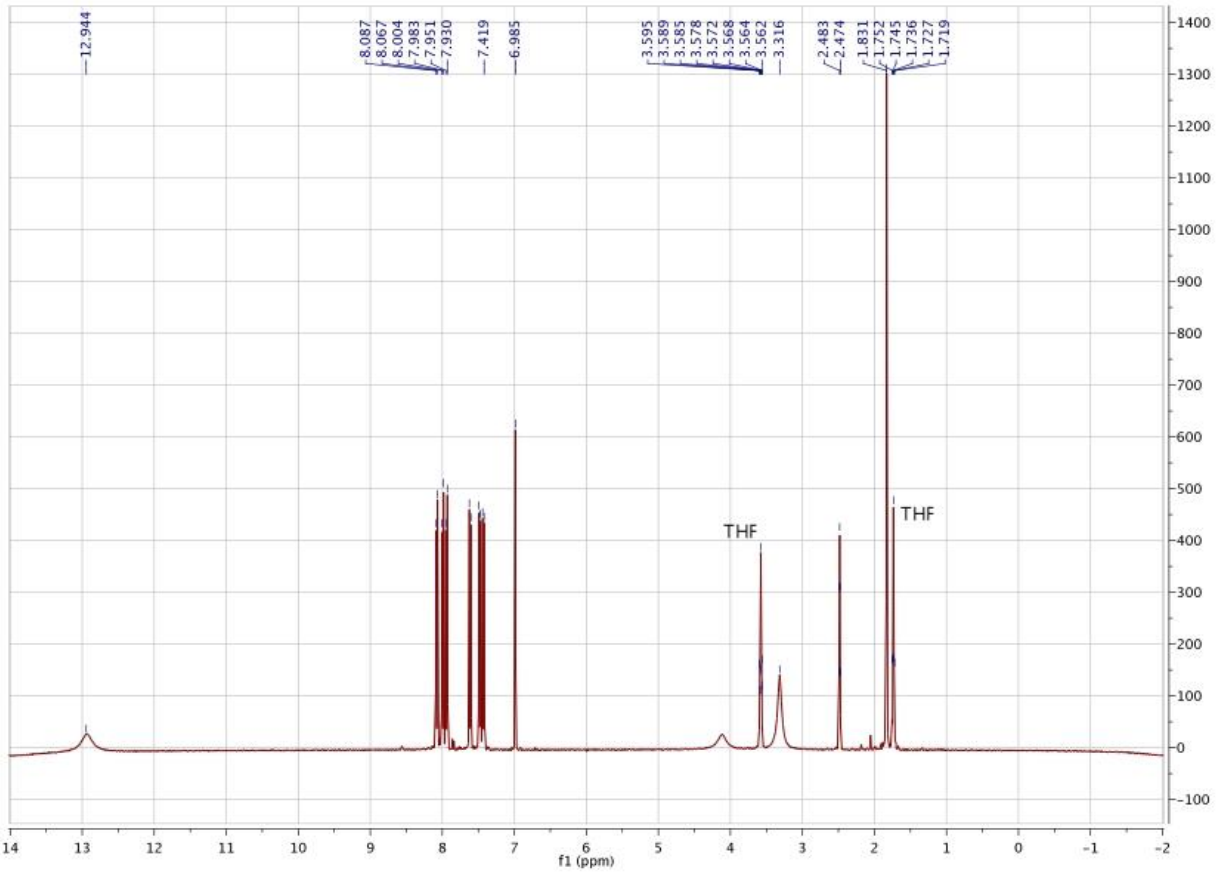

Figure S35. ^{1}H NMR (400 MHz, DMSO-d_6) of filtered and air-dried crystals of **6**.

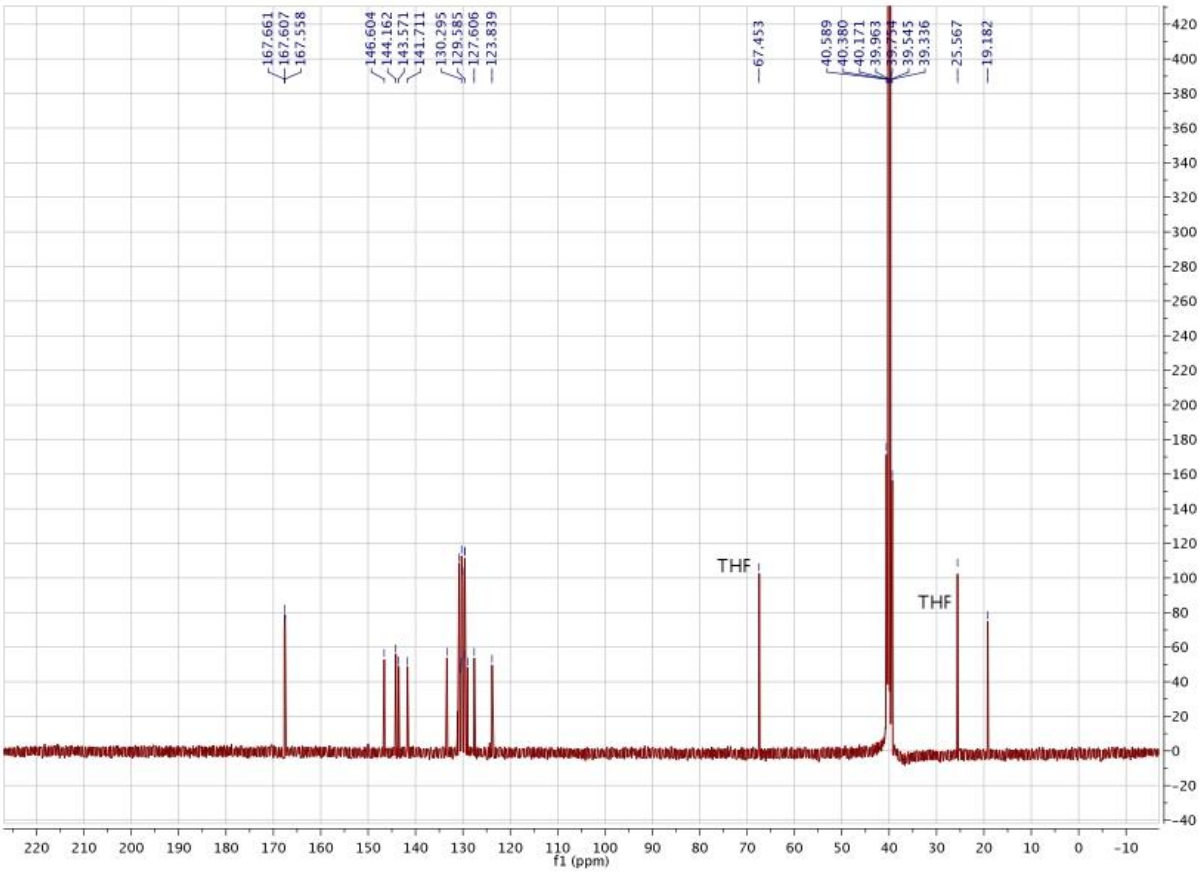

Figure S36. ^{13}C NMR (100 MHz, DMSO-d_6) of filtered and air-dried crystals of **6**.

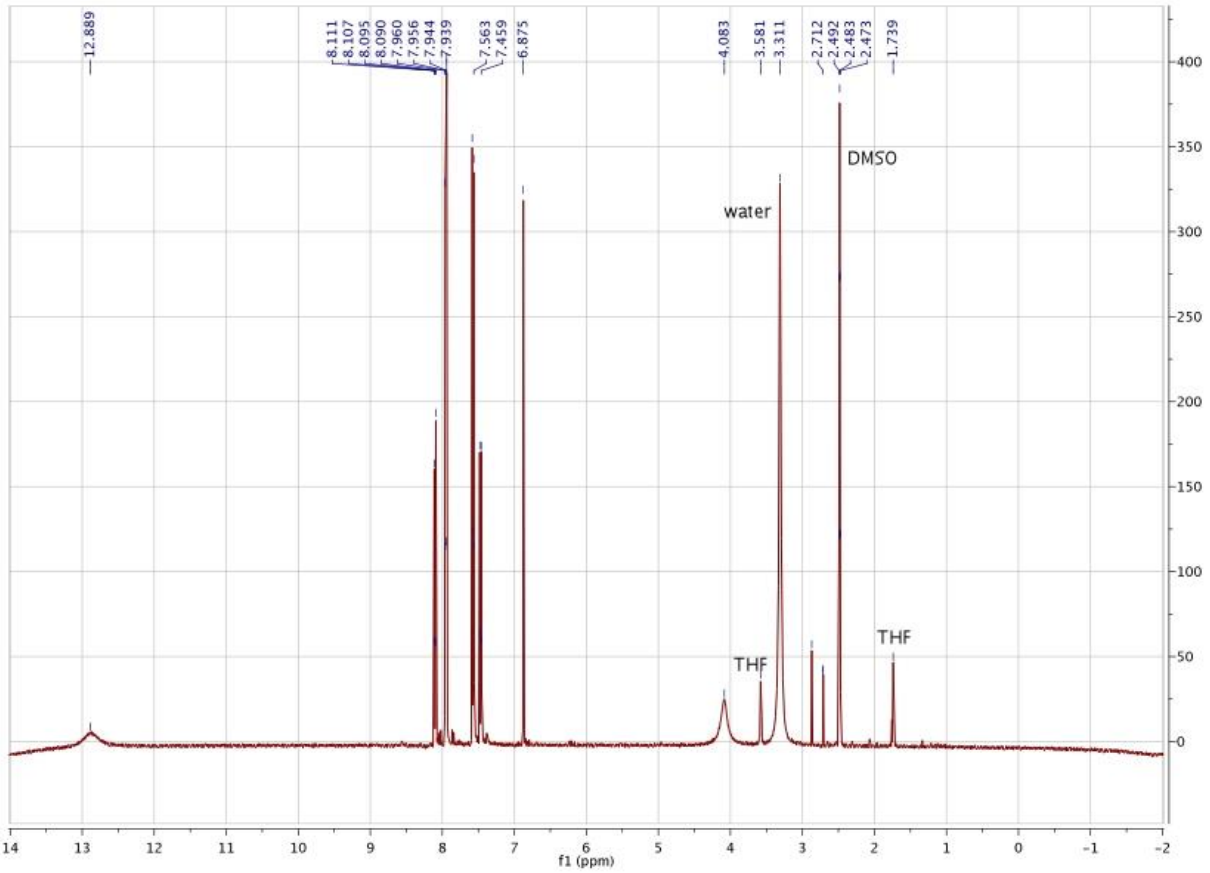

Figure S37. ^{1}H NMR (400 MHz, DMSO-d_6) of filtered and air-dried crystals of **7**.

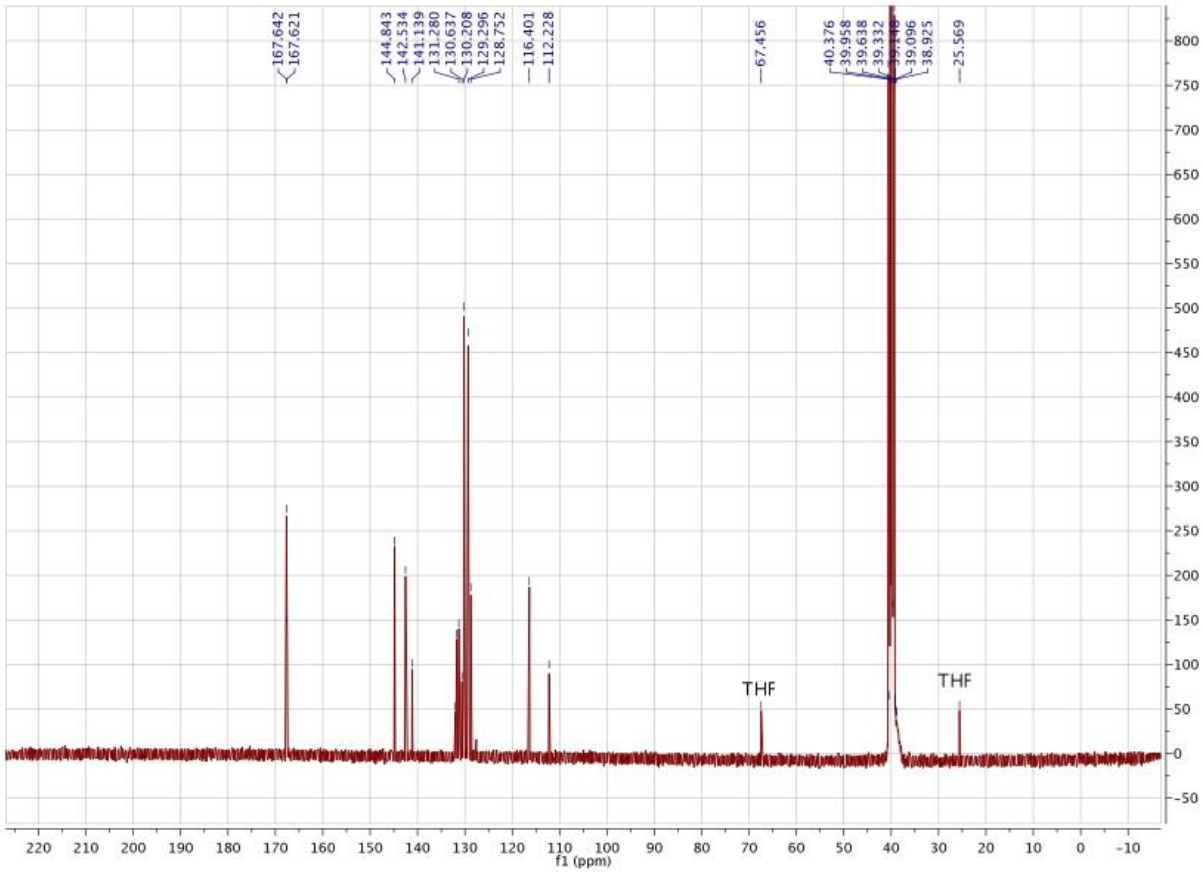

Figure S38. ^{13}C NMR (100 MHz, DMSO-d_6) of filtered and air-dried crystals of **7**.

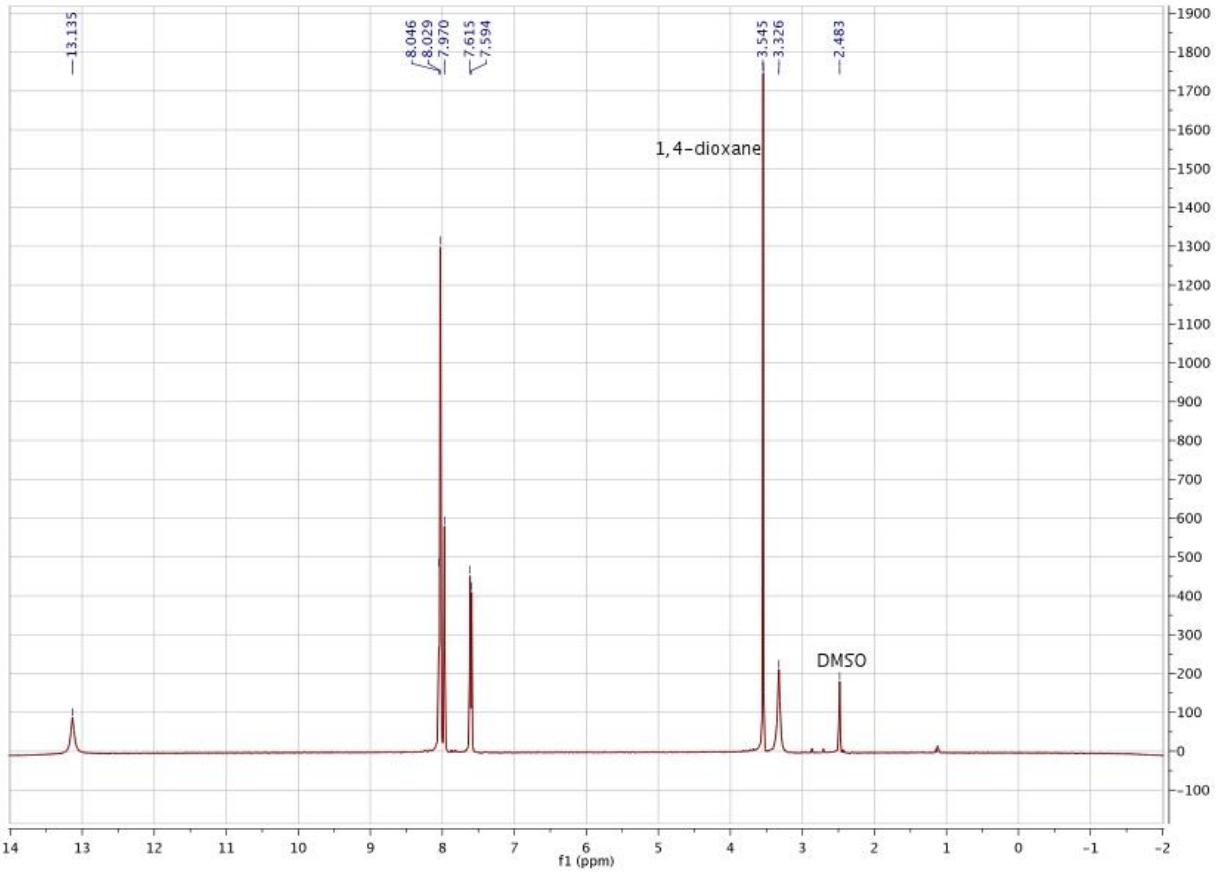

Figure S39. ^{1}H NMR (400 MHz, DMSO-d_6) of filtered and air-dried crystals of **8**.

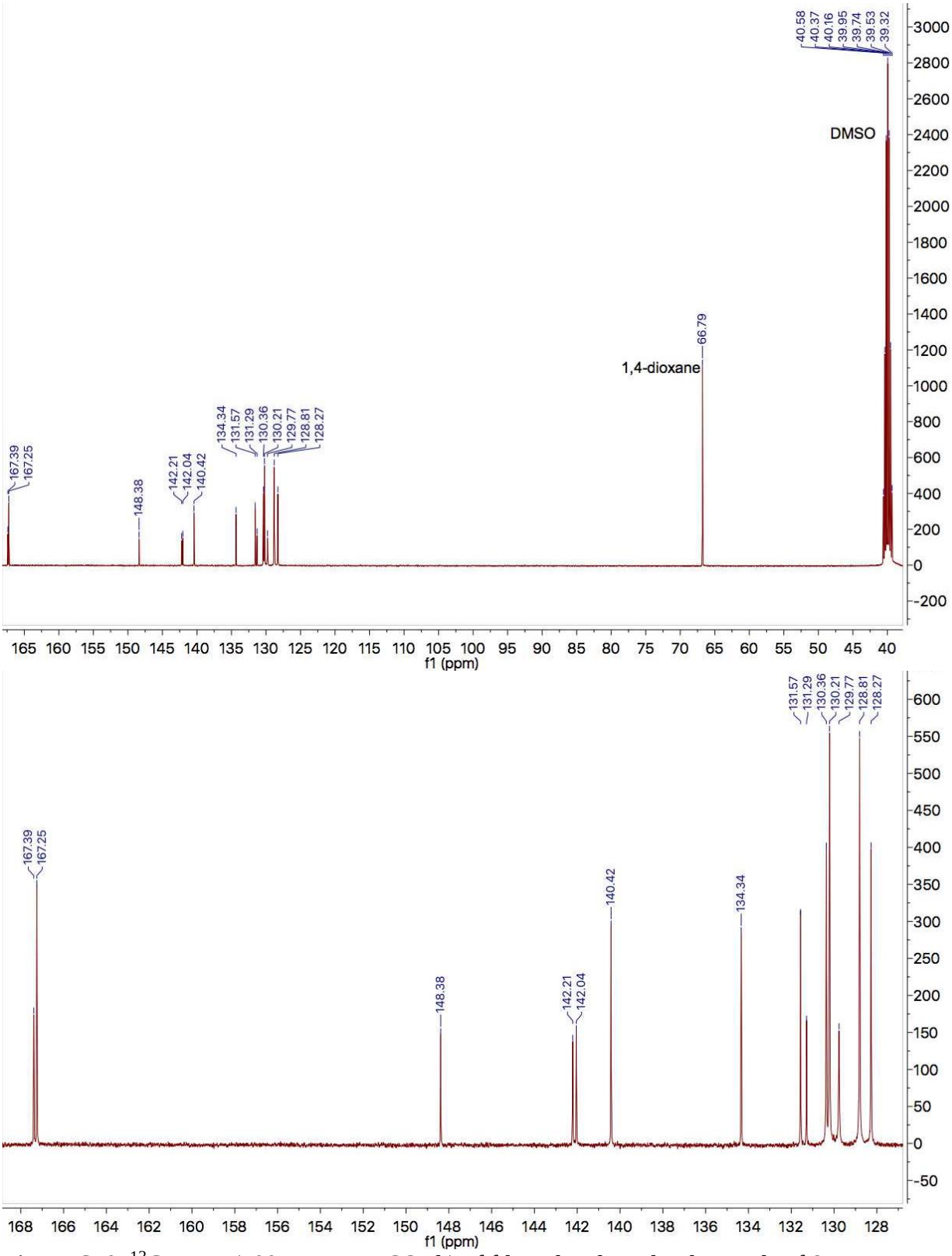

Figure S40. ^{13}C NMR (100 MHz, DMSO-d_6) of filtered and air-dried crystals of **8**.

Torsion Angles and Steric A Values

Torsion angles were measured using the Mercury software of the Cambridge Structural Data Centre. Some compounds have more torsion angles because of their higher number of asymmetric units.

Table S2. Steric A values of functional groups on the central ring of **1** and the torsion angles between the central and outer arene rings. Torsion angles given are for the *I2* polymorph.

	A Value	Torsion Angle
	0 (hydrogen)	34.78
	0 (hydrogen)	35.44
	0 (hydrogen)	18.09
		38.9
		26.66
		27.84
		35.17
		37.63
		26.45
		26.24
		31.5
		26.66
		30.38
		28.08
		36.5
		38.48
		34.19
		32.6
		27.64
		27.91
		35.04
		36.13
		40
		39.72
		38.03
		39.29
		35.85
		35.28
		28.67
		30.88
		37.28
		35.95
		43.41
		41.87
		28.8
		26.78

		36.68
		39.03
		25.98
		26.55
		43.41
		45.1
		27.98
		27.04
		33.2
		34.7
		42.44
		39.96
		29.83
		26.98
		39.35
		39.32
		33.27
		32.53
		29.19
		27.97
		34.11
		34.27
		39.91
		38.57
		36.57
		38.91
		31.48
		29.36
		22.85
		23.85
		30.89
		28.83
		39.18
		40.46
		36.75
		33.73
		31.65
		32.65
		49.32
		38.99
		27.99
		29.86
		41.44
		41.47
		33.05

		33.81
		27.24
		26.67
average	0	33.67

Table S3. Steric A values of functional groups on the central ring of **2** and the torsion angles between the central and outer arene rings.

	A Value	Torsion Angle
	1.7 (methyl)	1.08
	0 (hydrogen)	60.21
	0 (hydrogen)	61.37
average	0.57	40.87

Table S3. Steric A values of functional groups on the central ring of **3** and the torsion angles between the central and outer arene rings.

	A Value	Torsion Angle
	0.6 (methoxy)	30.65
	0 (hydrogen)	36.27
	0 (hydrogen)	31.69
		33.43
		39.62
		40
		21.93
		20.34
		46.06
		44.16
		45.19
		46.68
		23.14
		26.27
		40.08
		45.84
		44.96
		38.46
average	0.20	36.38

Table S5. Steric A values of functional groups on the central ring of **4** and the torsion angles between the central and outer arene rings.

	A Value	Torsion Angle
	0.6 (methoxy)	64.29
	1.6 (methyl)	64.18
	0 (hydrogen)	52.1
		55.36
		51.59
		45.5
		49.29
		49.16
		48.26
		55.49
		62.65
		64.51
average	0.77	55.20

Table S6. Steric A values of functional groups on the central ring of **5** and the torsion angles between the central and outer arene rings.

	A Value	Torsion Angle
	1.6 (amino)	2.56
	0 (hydrogen)	2.56
	0 (hydrogen)	50.34
		51.79
		0.84
		0.84
		50.67
		47.87
		1.89
		1.89
		53.37
		50.03
		50.34
		51.79
		50.67
		47.87
		53.37
		50.03
average	0.53	36.38

Table S7. Steric A values of functional groups on the central ring of **6** and the torsion angles between the central and outer arene rings.

	A Value	Torsion Angle
	1.7 (methyl)	53.71
	1.6 (amino)	56.09
	0 (hydrogen)	69.87
		71.87
		46.86
		52.18
average	1.1	58.43

Table S8. Steric A values of functional groups on the central ring of **7** and the torsion angles between the central and outer arene rings.

	A Value	Torsion Angle
	1.6 (amino)	59.11
	1.6 (amino)	60.13
	0 (hydrogen)	52.3
		58.17
		64.75
		68.46
average	1.07	60.49

Table S9. Steric A values of functional groups on the central ring of **8** and the torsion angles between the central and outer arene rings.

	A Value	Torsion Angle
	1.1 (nitro)	3.08
	0 (hydrogen)	1.94
	0 (hydrogen)	61.37
		53.01
		51.91
		59.6
		49.63
		51.98
		41.33
		37.91
		48.96
		50.78
average	0.37	42.63

Table S10. Steric A values of functional groups on the central ring of **9** and the torsion angles between the central and outer arene rings.

	A Value	Torsion Angle
	1.7 (methyl)	83.07
	1.7 (methyl)	85.01
	1.7 (methyl)	87.67
		93.82
		88.62
		87.77
average	1.7	87.66